J. Phys. C: Solid State Phys. **18** (1985) 3839–3871. Printed in Great Britain

REVIEW ARTICLE

Irradiation-induced defects in GaAs

D Pons†§ and J C Bourgoin‡

†Laboratoire Central de Recherches, Thomson–CSF, 91401 Orsay, France

‡Groupe de Physique des Solides de l'ENS, Tour 23, Université Paris VII, 2 Place Jussieu, 75251 Paris Cedex 05, France

Received 17 December 1984

Abstract. From a discussion of the experimental results concerning defect creation (versus the energy of irradiation, temperature, doping concentration, nature of the material, crystalline orientation) and annealing (versus doping concentration, carrier injection), it is concluded that the defects produced in n- and p-type GaAs by electron irradiation consist in a distribution of vacancy–interstitial pairs in the As sublattice. The vacancy–interstitial pairs in the Ga sublattice recombine immediately after their creation. The mobility of the As interstitial, which can be induced by hole injection in the case of irradiation with high fluxes, explains the formation of antisites As_{Ga} by exchange with donor impurities on Ga sites and of few complexes following irradiations at high fluences. The existence of several types of pairs explains the occurrence of the numerous electron and hole traps observed. The electrical and optical characteristics of the electron traps are consistent with the existence of a strong electron–lattice coupling which can be evaluated semiquantitatively.

1. Introduction

The study of defects is one of the current problems in semiconductor physics. Theory is now able to predict qualitatively the position of the energy levels associated with ideal simple intrinsic defects, such as the unreconstructed vacancy, or impurities (Lannoo and Bourgoin 1981). However, it is not yet able to account quantitatively for the lattice distortion and relaxation which occur around such defects, although the 'negative-U' character of some defects has been predicted (Baraff *et al* 1980). In order to test the validity of these theoretical predictions, the experimentalists must produce these simple defects, identify them and then measure their characteristics.

The need to solve this problem is well illustrated by the fact that most of the electronic properties of a material and, consequently, the performances of the devices made with it depend ultimately on the presence of the defects. Thus, the logical first step to master the effect of a defect on electronic properties should be its identification. It is for instance doubtless that the identification of the so-called EL2 defect in GaAs would lead to rapid progress in the technology of this material.

The most interesting defects from the technological point of view are those created by the various thermal and mechanical stresses involved in device processing. However,

§ Present address: Département d'Instrumentation Nucléaire, Enertec Schlumberger, Parc des Tanneries, 67380 Lingolsheim, France.

0022-3719/85/203839 + 33 $02.25

since the intrinsic defects are then created at temperatures at which they are presumably very mobile, the resulting defects are complexes of these intrinsic defects with voluntary or non-voluntary contaminant impurities. Thus the study of such defects is necessarily complicated and provides information on the interactions of intrinsic defects with impurities or with extended defects such as dislocations, more than on the intrinsic defects themselves.

In contrast, irradiation, specially electron irradiation, is an easy way to introduce simple intrinsic defects, i.e. vacancies and interstitials, in controlled quantities (Bourgoin and Lannoo 1983, ch 8). This is due to the fact that the impinging electrons in the range 0.1–1 MeV carry just enough kinetic energy to displace one single atom in one collision event with the atoms of the solid. As nuclear reaction does not take place in this energy regime, the kinetic energy and momentum are conserved during these elastic collisions so that the total number of displaced atoms can be quantitatively predicted. Moreover, the electron energy losses are such that the displacements are created homogeneously at a rather large depth (~0.1 mm at 1 MeV). In addition, since the impinging electrons conserve their initial direction for a few μm inside the crystal, it is legitimate to study the dependence of the beam orientation with respect to the crystal orientation, in order to obtain information on the creation mechanism and, consequently, on the nature of the displacement in a compound. Finally, since it is possible to perform an irradiation at very low temperature, it is possible in principle to prevent the diffusion of the defects created from taking place. The displaced atom, i.e. the interstitial, can be expected to remain in the vicinity of its initial, unoccupied lattice site, i.e. the vacancy, thus forming a Frenkel pair. Raising the temperature of the material will have the effect of allowing the elements of these pairs to move, resulting in their recombination or in their dissociation. Those which escape recombination will be able eventually to interact with impurities giving rise to complex defects.

The defects introduced by irradiation in GaAs have been the subject of a considerable amount of work (for previous reviews, see Mircea and Bois 1979, Lang 1977). Electron irradiation has mainly been used because, as said above, it is an easy way to produce vacancies and interstitials in both sublattices, and to follow their transformation when they become mobile and interact with each other and, eventually, with the various impurities contained in the material. Ion irradiation has also been used. Complications then arise because the mass of the particle enables it to displace a large number of lattice atoms, i.e. to produce clusters of defects. The defects introduced by proton or neutron irradiation or ion implantation and those remaining after annealing have not been so extensively studied; see however, the recent review by Martin and Makram-Ebeid (1983).

Despite the numerous studies so far undertaken, very few simple intrinsic or complex defects have yet been firmly identified. The reason for this is that a direct identification can only be provided by electron paramagnetic resonance (EPR) (Bourgoin and Lannoo 1983, ch 3) which is difficult to perform in this material. This is due mostly to the fact that the hyperfine interactions, which are of large magnitude, cannot be easily resolved because all the isotopes possess the same nuclear spin, $\frac{3}{2}$ (^{75}As 100% abundant, ^{69}Ga 60% abundant, ^{71}Ga 40% abundant) and the linewidths are large compared with the superhyperfine splitting. This is the main reason for which so few defects have been identified in III–V compounds compared with II–VI compounds (where the strength of the hyperfine interaction is much less) and silicon (where the situation is ideal with only ^{29}Si, 5% abundant, possessing a nuclear spin). However, as we shall see, some defects have been detected with this technique (such as the antisite) and there is some hope that

spin resonance could be detected by combination with a more sensitive technique (such as deep-level transient spectroscopy), optical detection of magnetic resonance or of electron–nuclear double resonance.

The other technique which can allow direct identification of a defect is infrared absorption on localised vibrational modes (Lannoo and Bourgoin 1981, ch 5), but it applies only to light impurities. As we shall see, it has produced significant information on the association of primary defects with impurities, i.e. indirectly on the behaviour of these primary defects.

The other optical techniques: luminescence and infrared absorption (Bourgoin and Lannoo 1983, ch 4) are not very well adapted to study irradiation-induced defects. Luminescence is a powerful tool for detecting and identifying shallow impurities, but its efficiency decreases rapidly when deep levels are introduced because they often act as effective non-radioactive recombination centres. As to infrared absorption, it provides broad bands and not sharp lines (Pajot 1984) because, as we shall see, a strong electron–lattice coupling (Bourgoin and Lannoo 1983, ch 2) is associated with deep defects in gallium arsenide.

Therefore, in order to identify and study intrinsic defects, one must rely mostly on indirect ways, in which spectroscopic techniques such as optical absorption or luminescence and electrical techniques (Hall effect and transient techniques monitoring the emission rate of carriers from defect levels towards the bands) are used to determine the behaviour of the defects versus various parameters. The dependence of the concentration of each defect detected by these techniques on the parameters characterising (i) the material (nature of dopant impurities, concentration of free carriers, eventually the composition in ternary alloys such as $Ga_{1-x}Al_xAs$ or GaP_xAs_{1-x}); (ii) the irradiation (energy, temperature of irradiation, orientation of the beam as compared with the crystallographic directions); and (iii) annealing (temperature, charge state of the defects, minority carrier injection) provides partial information which, when put together and compared with some theoretical predictions, should hopefully allow one to deduce the nature of the defects involved.

The aim of this paper is to collect all the available data in the literature, providing on some occasions new results, and to present a critical discussion of them in order to propose an identification for some of the most important defects observed. In particular, it will be shown that the identification of several levels with different configurations of the vacancy–interstitial pair in the As sublattice is reasonable. Because the question is not yet resolved, it is still the subject of much investigation. A number of conclusions have been proposed that are justified by unpublished results not detailed here.

The paper is divided into four parts. Section 2 deals with the introduction of defects by irradiation. After a brief description of the defects introduced, we discuss their creation rates and corresponding orientation dependence. In n-type material we provide definitive results showing that three traps, the so-called E_1, E_2 and E_3 traps, at least, are directly produced by 4 K irradiation. This, coupled with the results of the anisotropy of defect creation, allows one to conclude that the observed defects are primary defects in the As sublattice (i.e. formed by immobile As vacancies, V_{As}, and As interstitials, As_i) and that no defects are present in the Ga sublattice. The situation is similar in p-type material. Complexes such as association of As_i with B and C and antisites As_{Ga} are also formed following room-temperature irradiation in particular conditions. We shall examine them and discuss a possible mechanism by which the antisites As_{Ga} and the complexes are formed.

Section 3 is devoted to defect annealing. After a brief description of the thermal

behaviour of the defects, the annealing kinetics and the influence of the presence of doping impurities are discussed. Again, the type of kinetics observed, as well as the formation of complex defects during irradiation at high temperature, is consistent with the fact that the defects observed in n-type material are vacancy–interstitial pairs.

Finally, in §4, we shall see how the characteristics of the identified defects: capture cross-sections for majority carriers, optical cross-sections, energy level positions in the forbidden gap, Franck–Condon shifts, etc, can be understood in terms of available theories. This will lead us to the conclusion that although we understand correctly which defects are formed and how they are formed, much more remains to be done before the subject will be closed. For this reason, all through the paper, we suggest experiments we feel are necessary to improve the situation.

2. Production by irradiation

2.1. Description

We adopt the classification of Lang and Kimerling (1974). Following electron irradiation, eight electron traps, labelled E_1–E_5, E_7–E_9 and three hole traps H_1–H_3 are detected in n-type material. Typical spectra for the traps E_1–E_5 and H_1–H_3 have already been given by Lang (1974). The trap E_8 was also observed by these authors but not labelled and ignored because of its small concentration. The traps E_7 and E_9 are observed only after low-temperature irradiation ($T < 200$ K), results to be discussed later in this section. We give in figure 1 a typical spectrum obtained after a 4 K irradiation exhibiting these traps in addition to the usual E_1–E_3 traps. We shall not consider the trap E_6 which has been observed only on one series of Schottky diodes irradiated after the barrier (gold) was evaporated (Pons *et al* 1980a). All these traps are easily observed using deep-level transient spectroscopy (DLTS) (Lang 1974, Bourgoin and Lannoo 1983, ch 6) when enough care is taken to avoid the enhancement of the emission rate from the electron traps by the electric field (see §4.5).

The H_1 to H_3 traps (traps H_2 and H_3 have also been labelled A and B, respectively) have also been observed in p-type material (Lang and Kimerling 1975, Loualiche *et al* 1982b) with an additional trap H_0 (Pons 1983): see figure 2. This last trap, which is in

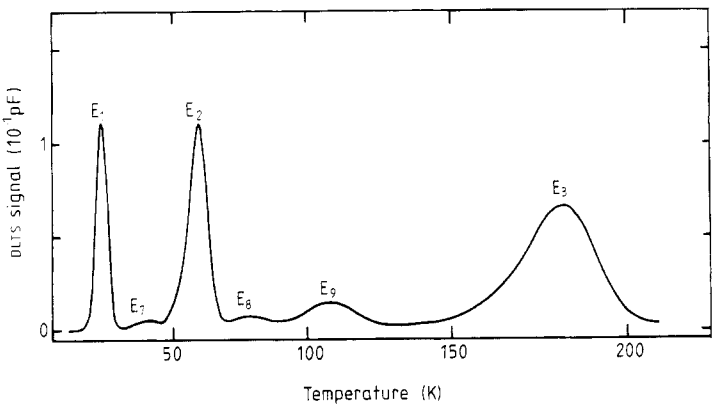

Figure 1. DLTS spectrum in an n-type VPE layer irradiated with 5×10^{13} cm^{-2}, 1.5 MeV electrons at 4.2 K.

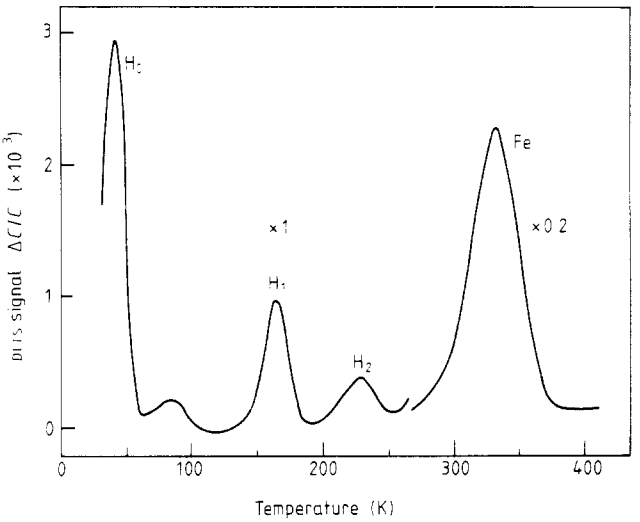

Figure 2. DLTS spectrum in a p-type VPE layer irradiated with 3×10^{15} cm^{-2}, 1 MeV electrons at 300 K.

fact the most important hole trap, is not observed in n-type material but could eventually be present, but undetected for various reasons (masked by one of the electron traps, for instance). However, in this type of material the situation seems *a priori* more complicated than in n-type material. Indeed, in n-type material the traps observed do not depend on the quality of the material, i.e. on the way it has been grown (vapour- or liquid-phase epitaxy, Czochralski, etc) nor on the nature and concentration of the doping impurities it contains. This is not the case in p-type material where traps other than the H_0–H_3 traps, whose nature depends apparently on the quality of the layer, can be present (Loualiche *et al* 1982b). This fact suggests, therefore, that the defects created by the irradiation do not behave the same way in n-type as in p-type materials. Finally, it is not possible to know whether the E and H traps are associated with the same defects since, unfortunately, the detection of the E traps has not yet been attempted in p-type material. Therefore we do not know whether these E traps are really present after irradiation in this type of material.

The E traps are always introduced with the same introduction rate in n-type material, whatever the concentration and nature of the impurities (Kolchenko and Lomako 1978) and of the native defects it contains. This constitutes a first strong indication that these traps should correspond to stable intrinsic defects since they do not interact with the various impurities contained in the material. On the contrary in p-type material, some of the introduced traps (other than the H_0–H_3 traps) are different in LPE and VPE layers, indicating that some of the primary defects interact with impurities, i.e. are mobile (at least at room temperature, the temperature at which the irradiation in this type of material was performed). Only the introduction rates of the H_0 and H_1 traps have been measured following 4 K irradiation (Pons 1983). Because these rates are practically the same for 4 K as for room-temperature irradiation, it is reasonable to conclude that the H_0, H_1 traps are also related to primary defects. The reason for which some other traps, related to impurities, can be formed will be discussed in §2.4.

The temperatures at which the carriers are emitted from these E and H traps towards the conduction or valence bands, for a typical emission rate of $\sim 10^2$ s^{-1}, are given in

Table 1. Peak temperature T_0 (for an emission rate of 70 s^{-1}), introduction rate τ for 1 MeV irradiation, energy level E_e (from the conduction band), apparent capture cross-section σ_a (deduced from the extrapolation to $T^{-1} = 0$ of the Arrhenius plot of the emission rate), annealing temperature T_a, activation energy associated with the annealing E_a, pre-exponential factor of the annealing rate ν, Franck–Condon shift d_{FC} and activation energy ΔE associated with the capture cross-section for the traps observed by DLTS in n-type material.

Trap	T_0 (K)	τ (cm^{-1})	E_e (eV)	σ_a (cm^{-2})	T_a (K)	E_a (eV)	ν (s^{-1})	d_{FC} (eV)	ΔE (eV)
E_1	20	1.5	0.045	2.2×10^{-15}	500	1.55 – 1.6	$10^{13.5} - 10^{12.5}$	0.38	—
E_2	60	1.5	0.14	1.2×10^{-13}	500	1.55 – 1.6	$10^{13.5} - 10^{12.5}$	0.22	~0
E_3	160	0.4	0.30	6.2×10^{-15}	500	1.55	$10^{13.5}$	0.2	0.08
E_4	310	0.08	0.76	3.1×10^{-14}	500	1.5	10^{13}	—	—
E_5	360	0.1	0.96	1.9×10^{-12}	500	1.55	$10^{13.5}$	—	—
E_7	40	$\sim 5 \times 10^{-4}$	—	—	250	0.7	10^{12}	—	—
E_8	80	$\sim 5 \times 10^{-4}$	—	—	—	—	—	—	—
E_9	110	$\sim 2 \times 10^{-3}$	—	—	250	0.7	10^{12}	—	—
P_1	200	$\sim 10^{-2}$	0.36	6.9×10^{-15}	—	—	—	—	—
P_2	280	$\sim 10^{-2}$	0.50	1.4×10^{-15}	—	—	—	—	—
P_3	350	$\sim 10^{-2}$	0.72	1.4×10^{-13}	620	1.5	10^9	—	—

Table 2. Peak temperature T_0 (for an emission rate of 70 s^{-1}), introduction rate τ for 1 MeV irradiation, energy level E_e; from the valence band), apparent capture cross-section σ_a and annealing temperature T_a for the traps observed by DLTS in p-type material.

Trap	T_0 (K)	τ (cm^{-1})	E_e (eV)	σ_a (cm^{-2})	T_a (K)
H_0	50	0.8	0.06	1.6×10^{-16}	—
H_1	150	0.1 – 0.7	0.29	5×10^{-15}	500
H_2	190	—	0.41	2×10^{-16}	—
H_3 (B)	340	~0.2	0.71	1.2×10^{-14}	—

tables 1 and 2 for electron and hole traps, respectively. Because the detection of defects by DLTS implies the use of a thermal scan, it is not *a priori* obvious that the defects are directly created by 4 K irradiation. In order to show that E_1, E_2 and E_3 are indeed present after 4 K irradiation we have proceeded as follows. The electron irradiation has been performed with the samples at 4 K in a cryostat, through a thin (~30 μm) stainless steel window. Figure 1 displays the DLTS spectrum recorded just after 4 K irradiation during the first thermal scan in a sample containing 2×10^{16} cm^{-3}, free electrons and before any annealing has taken place. This spectrum exhibits the usual E_1, E_2 and E_3 traps; it also shows additional traps, not reported up to now, E_7 and E_9 in low concentration (we have recently learnt that E_9 has been detected by Razazadeh and Palmer (1985)), about 20 times lower than the concentration of E_2 (as we shall see in §3, the E_7 and E_9 traps are not stable at room temperature). In principle, the E_1, E_2 and E_3 traps are observed at, respectively, ~20, 50 and 160 K. However, a special property of these defects, namely that their emission rate can be greatly enhanced by phonon-assisted tunnelling (see §4.5), allows E_1 and E_2 to be observed at 4 K. By using an adequate value of the electric field in the junction, it can be arranged for their emission rates to be easily measured

and separated at this low temperature. The observation is performed in the following way: a filling pulse is applied to the diode and the resulting capacitance transient is recorded. From the time and pulse-amplitude dependences of the transient and using the results of a previous study of the effect of an electric field on E_1 and E_2 (D Pons, unpublished), we were able to conclude that both E_1 and E_2 are present just after the 4 K irradiation. A similar experiment was performed at a higher temperature (80 K) which shows that E_3 exists already at this temperature (the contribution of E_1 and E_2 to the capacitance transient prevents the detection of E_3 at a lower temperature).

We have looked for a possible effect of the Fermi level position on the introduction rates of E_1, E_2 and E_3 by comparing the results obtained for irradiation at 4 K with and without a reverse bias applied to the diode: *no dependence* has been detected. For this type of experiment the intensity of the irradiation beam has been kept low enough ($\sim 0.1\ \mu A\ cm^{-2}$) to ensure that the free-carrier concentration is not perturbed by the electron–hole pairs injected by the beam. Only a weak flux dependence, if any, was observed for the introduction rates of E_1 and E_2 in the range 0.1–5 $\mu A\ cm^{-2}$. We shall see the implication of this result in § 2.4.

We have also checked that the introduction rates of E_1 and E_2 do not depend on the temperature between 4 and 300 K. In order to obtain the concentrations of these traps accurately we have monitored the amplitude $\Delta C(\Delta V)$ giving directly the trap concentration (Lang 1974, Pons 1984b). The curves $\Delta C(\Delta V)$ are identical for both E_1 and E_2; only the saturations of the amplitudes differ because the effect of the electric field on the emission rates (see figure 3) is stronger for E_1 which has the shallowest energy level. Thus, the E_1 and E_2 traps are very probably associated with the same defect.

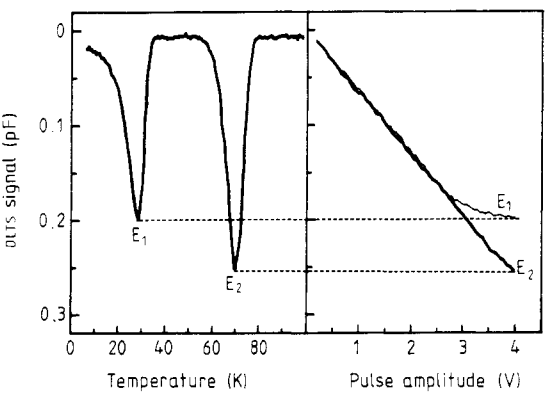

Figure 3. Typical DLTS spectrum showing the E_1 and E_2 traps (reverse bias 4.5 V; amplitude of the filling pulse 4.5 V) and variation of the amplitude of the peaks versus the amplitude of the filling pulse.

2.2. Introduction rates

The concentrations of the various majority carrier traps (traps E in n-type and H in p-type materials) can be accurately determined using the DLTS technique.

A compilation of the published results is given in tables 1 and 2 for a typical electron energy (1 MeV). Clearly, in n-type material the introduction rates of the E traps are, within a 25% accuracy, always the same. As to the H traps, their introduction rates

cannot be measured correctly in n-type material because the concentration of the minority carriers which has to be injected in order to observe them cannot be known accurately. In p-type material there is a large scatter in the values obtained for the H traps. This scatter, as well as the presence of various other traps (Loualiche *et al* 1982b) in variable concentrations, suggests that in p-type material some hole traps at least are associated with complexes of primary defects with impurities (the variable concentration of these impurities could explain the observed scatter on the introduction rates of the H traps).

In order to compare the observed introduction rates with the number of displacements produced, it is necessary to know the threshold energy, i.e. the minimum energy transmitted to a lattice atom to produce a displacement (Bourgoin and Lannoo 1983, ch 8). This threshold energy T_d is determined by fitting the experimental variation of the introduction rate of a defect versus the energy of irradiation to that calculated as a function of T_d.

Various determinations of T_d have been attempted. The early ones used resistivity measurements or luminescence to monitor the defect introduction rate versus electron energy. The results present a rather large scatter (from 9 to 15 eV) presumably because the techniques used are not well adapted to such determination (for a review, see Corbett and Bourgoin (1975)). Indeed, resistivity measurements necessitate thick samples through which the electron energy varies and is sensitive to surface states. Luminescence, which can also be sensitive to surface effects, is only an indirect method since the defects introduced are mainly non-radiative and damp the luminescence efficiency. In contrast, DLTS, a technique that is well adapted since it allows the concentration of the defects in a thin layer below the surface ($\sim 1\ \mu$m) to be measured, provides more reliable results.

The threshold value obtained by DLTS is found to be $T_d = 9$–10 eV for traps E_1–E_5 and H_0, H_1 (Pons *et al* 1980b, Pons 1983). For such a value, the total defect introduction rate expected is, at 1 MeV, $\sim 7\ \text{cm}^{-1}$ in one sublattice. However, other defects correspond to a threshold, approximately equal to $2T_d$. Thommen (1970) using resistivity measurements, distinguished three types of defects (classified as stages I, II and III from their annealing behaviour): type I and II defects, which anneal below room temperature, correspond to a higher threshold ($\sim$20 eV) than type III defects (Pons *et al* 1980b) which anneal above room temperature. This observation of the existence of two thresholds is qualitatively confirmed by luminescence studies (Arnold and Gobeli 1968).

The type I or II defects are probably associated with the E_7 and E_9 traps since they have the same annealing behaviour (see § 3.1). Unfortunately, their threshold has not yet been determined by DLTS.

The comparison between the calculated introduction rate and the sum of the introduction rates of the various defects suggests, once again, that the defects are primary defects in n-type material. A threshold approximately two times higher than the threshold for atomic displacement T_d for the type I and II defects can be explained as follows: when the energy transmitted to the knock-on atom becomes larger than $2T_d$, this atom can in turn transmit its energy to a neighbouring atom and displace it. A double displacement occurs which corresponds to a defect composed of two adjacent vacancies ($V_{As} + V_{Ga}$) and of the two corresponding interstitials. This type of behaviour has been observed in silicon (Corbett and Watkins 1965) as well as in germanium (Poulin and Bourgoin 1980, 1981). In silicon it has been directly verified, using EPR, that the divacancy, when directly created, is indeed associated with a threshold $\sim 2T_d$.

The situation is less clear in p-type material where the H traps also correspond to the same threshold energy (Pons 1983). Because of several factors—no accurate deter-

mination of the introduction rates, apparent variation of the introduction rates with the type of material, variety of trap observed, presence or not of E traps—it is not easy to compare quantitatively the order of magnitude of the introduction rates with theory. However, the total introduction rate of the H traps alone is of the same order of magnitude as that of the E traps, suggesting that they should also be related to primary defects. The trap H_2 could be a particular case: its concentration is not uniform and increases when approaching the p/n^+ interface (Pons 1983), i.e. it could be a complex related to the donor impurity.

2.3. Orientation dependence of the introduction rate

Because incident electrons conserve the direction of the irradiation beam up to a few μm below the surface (in practice, for electrons having an energy in the range of interest, i.e. 200 keV to few MeV), the anisotropy of the probability of displacement which is expected in a compound material should be observed using DLTS since it is the technique perfectly adapted to probe the defects present in such a region. The anisotropy has its origin in the interaction of the primary knock-on atom with its nearest neighbours of different nature (Pons 1984a). For instance, as illustrated in figure 4, an As atom should

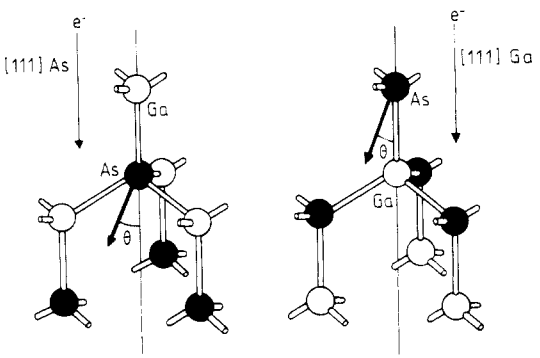

Figure 4. Diagram showing an As displacement for an irradiation along [111] As and [111] Ga directions. The angle θ is the recoil angle of the As atom in the collision.

be 'easily' displaced if the beam is oriented along a [111] As direction and also the beam energy is close to the minimum energy necessary to displace the As atom because, only in this case, is the recoil direction of the As atom close to the [111] As direction. The As displacement should be 'more difficult', i.e. the probability of displacement should be smaller, if the incident beam direction is [111] Ga. The experimental situation is complicated by the fact that, for energies higher than the minimum displacement energy, the direction of the recoil atom can take large angles with the direction of the incident beam and be close to a $[\bar{1}11]$, $[1\bar{1}1]$ or $[11\bar{1}]$ direction which are 'hard' directions for displacement. The consequence is that the anisotropy appears to reverse at high enough energies for which the recoil occurs preferentially with large angles.

This concept of anisotropy of displacement has been established experimentally first using resistivity measurements (Thommen 1968, Eisen 1964). It has been quantitatively analysed and the anisotropy reversal predicted only recently (Pons 1984a). The use of DLTS to measure this anisotropy (Pons 1983, Pons and Bourgoin 1981) provides the

following result: all the traps studied in n-type (E_1, E_2 and E_3) as well as in p-type materials (H_0, H_1) for which the study has been performed exhibit an anisotropy such that they must originate from the As sublattice. This conclusion was later confirmed by a study of the variation of the introduction rates of the E traps as a function of the composition in GaAlAs alloys (Loualiche *et al* 1982a).

The conclusion of a prior investigation by Lang *et al* (1977) that E_3 belongs to the Ga sublattice was wrong because the energy of irradiation was too large compared with the threshold energy so that the average recoil angle of the atom was far from zero.

The anisotropy of the other traps (E_4, E_5), although studied in less detail, is also consistent with an As displacement. Finally, this anisotropy has not been studied for the traps E_7 and E_9 and the other numerous traps observed in p-type material. This is unfortunate since if, as we discussed in § 2.2, traps E_7 and E_9 indeed correspond to double displacements, they should not exhibit any anisotropy.

2.4. Impurity interaction

Complex defects involving impurities are observed using infrared absorption and EPR measurements following room-temperature irradiation. Brozel and Newman (1978) and Woodhead and Newman (1981) have shown by looking at the localised vibrational modes of boron that a defect involving boron is formed by room-temperature irradiation, presumably a boron atom complexed with an interstitial. Later, because there appears to be a threshold in the dose of irradiation for which this defect is produced, which corresponds approximately to a situation where the free electrons are all compensated by the defects, it was argued that the formation of such defects is due to the fact that the mobility of the interstitial occurs when the Fermi level is lowered to a critical position allowing it to be trapped by impurities such as boron and carbon (Beall *et al* 1984). This interpretation will be discussed below.

Similarly, in p-type material, a complex involving chromium has also been identified (Whitehouse *et al* 1981).

Finally, the generation of antisites As_{Ga} has also been observed. Such antisites were first identified in semi-insulating (Wagner *et al* 1980), plastically deformed (Weber *et al* 1982) and neutron-irradiated (Wörner *et al* 1982) materials using EPR. Their identification is based on a comparison of the hyperfine parameters with that of the antisite P_{Ga} in GaP after appropriate scaling of the nuclear moments and of the wavefunctions of the unpaired electrons. This identification was later said to be confirmed by magnetic circular dichroism measurements (Meyer *et al* 1984). The As_{Ga} antisite was first detected following room-temperature irradiation in p-type material (Kennedy *et al* 1981) and, subsequently, in n-type material (Goswami *et al* 1981) when the dose of irradiation is large enough for the defects to compensate the free carriers.

Because the As_{Ga} antisite defect was observed to be produced before the $B–As_i$ complex defect began to grow, Beall *et al* concluded that the creation of the As_{Ga} antisite defect was not due to the capture of As interstitials, but of Ga interstitials by some grown-in (undetected) defects. The Ga interstitials were also assumed to be created by the irradiation and to be mobile in the conditions of the irradiation. Newman and Woodhead (1984) and Beall *et al* (1984) assume that the interstitials become mobile once the Fermi level is lowered under some critical energy. The fact that the stability or mobility of a defect is governed by its charge state is now widely recognised. This is the case for Ge and Si self-interstitials for instance (Bourgoin and Lannoo 1983, ch 9). However, this interpretation is here in contradiction with the following observations:

(i) most of the created defects (E and H traps) are associated with primary defects in the As sublattice (i.e. V_{As} and As_i), stable at 300 K whatever their charge states; (ii) as shown in § 2.2 the introduction rate of the E traps is independent of the Fermi level position; (iii) it has been shown by Pons (1983) that these defects are indeed more stable when the position of the Fermi level is lowered. Therefore, the results of Newman and Woodhead and of Beall *et al* require a different interpretation. We argue that the interstitials that give rise to the formation of antisites are As_i since the study of the anisotropy of defect formation (see § 3.3) indicates that all the defects observed belong to the As sublattice. The reason for which the As_i get mobile during the irradiation is certainly related to the so-called recombination-enhanced mechanism, to be discussed in § 3. It has been shown by Lang and Kimerling (1974) and Lang *et al* (1976) that, when minority carriers are injected, the E traps can anneal at temperatures as low as 300 K depending on the concentration of injected carriers. As was already noticed by Newman and Woodhead, such enhanced annealing can also occur during irradiation if the electron flux is large. The concentration of injected carriers ($\Delta n = \Delta p$) is approximately equal to $E\tau\varphi/Rw$ where E and φ are the irradiation energy and flux, R the range which is about 1 mm for 1 MeV electrons in GaAs, w the energy required to form an electron–hole pair ($w = 4.5$ eV in GaAs, Klein (1968)) and τ the lifetime. With $E \simeq 2$ MeV, $\varphi = 10^{14}$ $e^- cm^{-2} s^{-1}$ as in the experimental conditions of the irradiations of Beall *et al*, and $\tau \simeq 10^{-7}$ s, we find: $\Delta p \sim 5 \times 10^{13} cm^{-3}$ which is enough to cause some enhanced annealing of the E traps and in particular of E_3.

A possible evolution in the nature and concentration of the E traps using DLTS in n-type material irradiated with high fluxes has been looked for (D Stievenard and J C Bourgoin, unpublished). The concentrations of E_4 and E_5 relative to each other change with the flux and at least one new trap is observed. This observation suggests that the holes injected by the irradiation induce to some extent the mobility of the primary defects. Such irradiation-induced mobility also allows one to understand the variation of the carrier removal rate versus the concentration and nature of the doping impurities observed after high-fluence irradiations (Kalma *et al* 1973, Kalma and Berger 1972).

The complex defects B–As_i, C–As_i were observed in n-type material to begin to grow after a certain threshold in the total dose of irradiation. Let us show that the appearance of a threshold in the irradiation dose is in fact very natural for the creation of this kind of complex, independently of the exact microscopic mechanism inducing the mobility of the interstitial. Let us assume, as usual, that the rate of capture of the interstitial by some impurity, *during the irradiation*, is proportional to the concentration of interstitials. The concentration of interstitial C_i should then be given by:

$$dC_i/dt = k\varphi - \sigma C_t C_i$$

where k is creation rate for dissociating vacancy–interstitial pairs, φ the irradiation flux, C_t the concentration of trapping impurities and σ an unknown parameter (depending on the mobility of the interstitial). Let us assume for simplicity that C_t is much larger than C_i, so that we get:

$$C_i = (k\varphi/\sigma C_t)[1 - \exp(-\sigma C_t t)].$$

The concentration of interstitials therefore begins to grow linearly with the dose, but saturates after a time constant $\tau_s \simeq (\sigma C_t)^{-1}$. The concentration C_c of complex defects which are formed as a result of the capture of the interstitials by the impurities is simply given by:

$$dC_c/dt = \sigma C_t C_i$$

which gives:

$$C_c = k\phi[t - \tau + \tau_s \exp(-t/\tau_s)].$$

The linear growth of complex defects with the irradiation dose therefore begins after the steady concentration of interstitials is reached. A threshold D for the irradiation dose must appear, whose value depends on the nature and concentration of the trapping impurity which is simply given by:

$$D = k\varphi\tau_s.$$

Such a threshold should be observed for the creations of the B–As_i and C–As_i complex defects if they result from the migration of the As interstitial during the irradiation. Thus, a detailed study of the flux dependence of the creation rates of the B–As_i and C–As_i complex defects should be of great help to deduce the exact mechanism of their creations.

The interstitial mobility readily explains the formation of C or B–As_i complexes, but not the formation of As_{Ga}. The antisite cannot be formed directly by a collision replacement mechanism since the defect formed should then be $V_{As} + As_{Ga}$ which would probably be distinguished by EPR from the isolated As_{Ga}; moreover, the introduction rate should not vary with the type and concentration of the doping impurity. It cannot either be formed by the recombination of As_i on a V_{Ga} after a double displacement, because the competition for such recombination between Ga_i and As_i could not result in the high introduction rates which are observed in some cases. Beall *et al* (1984), using the fact that they observe the saturation of the antisite EPR signal, argue that As_{Ga} forms as a result of the interaction of mobile Ga_i with an undetected grown-in defect such as, for instance $V_{Ga} + As_{Ga}$. This does not explain why the antisite concentration at saturation is always found to be of the order of the initial free-electron concentration (Goswami *et al* 1981). We rather suggest (J von Bardeleben and J C Bourgoin, unpublished) that the way the antisites form is through the interaction of mobile As_i and of donor impurities. The trapped As_i exchange with the substitutional impurity on a Ga site leading to an interstitial impurity and an antisite. This explains why the As_{Ga} concentration at saturation is always of the order of the impurity concentration (between 10^{16} and 10^{18} cm^{-3}) and also the variation of the threshold dose D as a function of the sample nature (n- and p-types). Such a type of exchange mechanism between a self-interstitial and a substitutional impurity is observed in silicon by EPR following 4 K irradiation (Watkins 1965) and by infrared absorption following room-temperature irradiation (Brozel *et al* 1975). In GaAs no such direct evidence has yet been found.

2.5. Conclusion

The various studies of defect production by electron irradiation in n-type material provide several arguments that the traps observed correspond to primary defects, i.e. are related to vacancies and interstitials in the As sublattice: V_{As} and As_i.

The arguments are the following: first, the defects are produced at 4 K. This is directly verified for E_1 and E_2 but this should also be the case for the other E traps because their relative concentrations compared with the (E_1, E_2) concentration are always the same whatever the temperature of irradiation (up to room temperature). Secondly, the defects produced are stable even at room temperature; no interaction is observed with the various impurities contained in the material: the energy levels observed and their introduction rates are independent of the way the material is grown and of the nature of

the doping impurity it contains. Third, the measured total introduction rate is of the order of the rate expected from calculation. The exact introduction rate is difficult to evaluate by summing the introduction rates of each individual trap because several traps can be associated with the different energy levels of the same defect. Consequently, only an evaluation of the introduction rate by a factor of ~2 is possible. From resistivity, *C–V* measurements and summing the various traps detected by DLTS one obtains, for 1 MeV electrons a total introduction rate of ~5 cm^{-1} which therefore compares favourably with the expected one (7 cm^{-1}) for the As sublattice. Fourth, the introduction rates of all the traps have the expected orientation dependence for As displacements. Fifth, the traps E_1 and E_2, because they are always created exactly in equal concentration, should correspond to two different levels of the same defect.

Finally, complex defects are also formed by electron irradiation at 300 K when the flux is high enough to induce the migration of the primary defects through a carrier recombination-enhanced mechanism. Some As_i escape from recombination with V_{As} and migrate until they are captured by impurities like boron and carbon. Antisites are also formed, probably by the replacement of donor impurities on Ga sites by As_i.

The first important question this conclusion brings is: where are the defects originating from the Ga sublattice, which undoubtedly are also created? There are two possible answers: (i) the corresponding defects do not give rise to any level in the forbidden gap; (ii) the V_{Ga} and Ga_i pairs recombine immediately, even at 4 K. The second answer is more probable than the first one because it is difficult to conceive that both V_{Ga} and Ga_i, or the complexes they could form with impurities, will not be associated, for the various charge states they could take, with any localised levels. On the contrary, the recombination of vacancy–interstitial pairs even at low temperature is quite natural: it happens at 4 K in p-type Ge n-type Si (Bourgoin and Lannoo 1983, ch 9). Local density calculations (Baraff and Schluter 1984) strongly suggest that the recombination is due to Coulomb attraction since V_{Ga} and Ga_i are found to have opposite charge states whatever the position of the Fermi level.

In p-type material the situation is less clear than in n-type material because the amount of information is quite insufficient. For the same reasons as for the E traps, we think that the H traps (with the exception of H_2) also correspond to primary defects in the As sublattice; however there is as yet no careful quantitative verification of this. The fact that additional traps, whose nature depends on the material, are sometimes observed can be understood in the same way as the formation of the As_{Ga} antisite of the complexes B–As_i and C–As_i: namely, through the mobility of As_i induced by electron–hole pair injection.

We shall now examine in the next section how the annealing behaviour of these defects corroborates these conclusions.

3. Annealing

3.1. Description

According to Thommen (1970) the defects produced by electron irradiation in n-type material anneal in three stages: stage I at ~230 K, stage II around 280 K and stage III around 500 K. Annealing experiments using the DLTS technique show that traps E_7 and E_9 must be ascribed to stage I (figure 5) while all other electron traps (E_1 to E_5) anneal to stage III (Lang 1977, Pons *et al* 1980a). No trap having a thermal behaviour

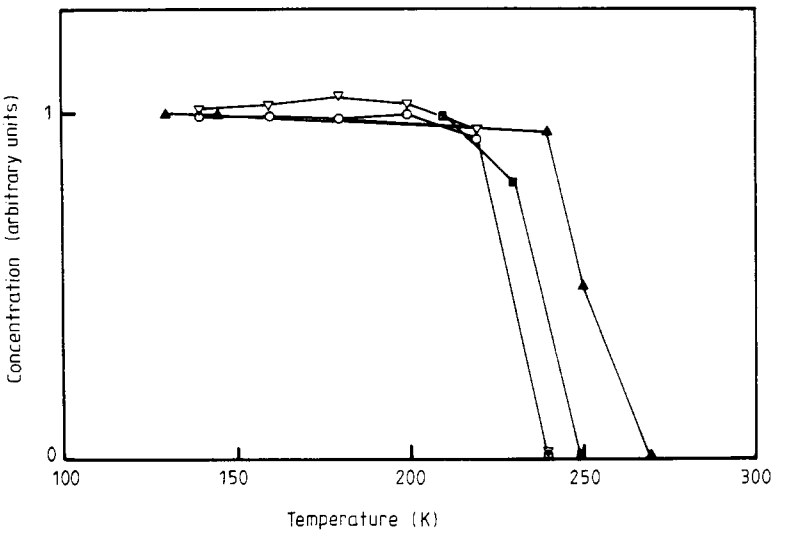

Figure 5. Isochronal annealing of the E_9 trap observed following 4 K irradiation by 1 MeV electrons (E_7 trap anneals in an identical fashion) in four different samples.

corresponding to stage II has been detected (this could be due to the fact that the corresponding traps are deep and anneal before they emit carriers in a band).

After stage III has been completed other traps appear, labelled P_1, P_2 and P_3 (Pons *et al* 1980a). The concentration of P_1 increases with the annealing temperature, around 500 K. Clearly, the appearance of the trap P_1 is correlated with the annealing of the primary defects. This is not so for P_2 and P_3. These traps are probably directly created by the irradiation, i.e. before any annealing has occurred (there is however a possibility that they result from the annealing in stages I or II). In both cases, it would be difficult to detect them before the annealing in stage III has occurred, because they are masked by E_4 and E_5. However, some numerical simulation of the DLTS spectra shows that they are indeed present just after the 300 K irradiation (D Pons, unpublished).

P_3 anneals around 650 K and P_2 at a slightly higher temperature (Pons *et al* 1980a). As to P_1, its possible annealing at a higher temperature has not yet been determined. Because the total concentration of the three traps P_1, P_2 and P_3 represents at most ~5% of the total E trap concentration present below 500 K, this implies that ~95% of the associated defects anneal in stage III.

Practically nothing is known about the thermal behaviour of each hole trap in n- and p-type materials. Only Lang (1977) has said that H_1 anneals in a similar fashion to E_3 and E_5, i.e. in stage III. Experiments performed using resistivity and Hall effect measurements in p-type material (Brailovskii and Brudnyi 1974) indicate that the main annealing stage in this material occurs around 500 K, i.e. presumably in stage III. If this stage is indeed the same for all H traps, this confirms that the defects related to H traps are the same as those related to the E traps, as already suggested.

As to the thermal behaviour of the complexes observed by infrared absorption, not much is known: the so-called B(1) centre (Özbay *et al* 1982), recently identified (see § 2.4) as a boron–interstitial complex, anneals in stage III. Obviously, since the kinetics are identical to the E_2 one, the annealing of B–As_i complexes occurs when the interstitial becomes mobile, which implies that the binding energy between As_i and boron is lower than the migration energy of As_i. Finally, a trap at $E_v + 0.51$ eV, tentatively ascribed to

a vacancy–Fe complex, appears following stage III annealing (Ikoma and Takikawa 1981).

These results are indirectly confirmed by luminescence (Arnold 1966, 1969, Barnes 1970, Ikoma and Takikawa 1981, Jeong *et al* 1973, Garrido *et al* 1981) and electrical (Farmer and Look 1980, Aukerman and Graft 1962) measurements. Some of these experiments were performed in compensated material (a doped material heavily irradiated), a case intermediate between the n- and p-type cases: stage III is observed but, when heavy particles are used to produce the defects, another stage—or several substages—are observed at higher temperatures (400–500°C). This is understandable in view of the fact that most of these defects are not simple intrinsic vacancies and interstitials. This could also be understood by considering the increased stability of the E defects when the Fermi level is lower than the E_3 level (see § 3.3).

3.2. Kinetics

Annealing kinetics has been studied carefully only for stage III in n-type material, for the sum of the defects (Farmer and Look 1980) by resistivity measurements and on each individual E defect by DLTS (Pons *et al* 1980a). Among the complexes, only the annealing kinetics of the B(1) centre has been studied: it is identical to the annealing of the E_2 trap (Özbay *et al* 1982).

Clearly all these traps anneal with the same activation energy (within the experimental accuracy) 1.5 to 1.7 eV (Lang *et al* 1976, Lang 1977, Pons *et al* 1980a) and the kinetics is first order. Only the E_2 trap (and the E_1 trap since both traps have to be attributed to the same defect, as shown in § 2.1) do not obey a simple first-order kinetics (Pons *et al* 1980a, Farmer and Look 1980): a fast annealing of a first fraction is followed by a slower decay. The total kinetics can be fitted by the sum of two first-order processes which both correspond to the same activation energy (they differ only by the pre-exponential factors). The annealing kinetics of the first fraction of E_2 is exactly identical to that of E_3, which strongly confirms that the associated defects, although different, have a common feature: their annealing should be driven by the *mobility of the same species*. The percentage of annealing in the first fraction seems to increase with increasing temperature and with the defect concentration. It seems likely that such behaviour is related to a change of Fermi level position as the annealing proceeds (see next section); however, we have not been able to check further this assertion.

3.3. Charge-state dependence

The effects of charge state on the annealing kinetics can easily be studied using the DLTS technique since a given thermal treatment can be performed with zero or reverse bias applied on the diode. First experiments led Lang and Kimerling (1974) and Lang *et al* (1976) to conclude that the annealing of the E and H_1 traps was not sensitive to charge-state effects. Consequently, Lang (1977) interpreted the dependence of the annealing rate of E_2 upon the doping concentration (Aukerman and Graft 1962) as a consequence of long-range diffusion of E_2 towards the dopant impurities. However, it was later demonstrated (Pons 1981) that a charge-stage effect is actually operative in stage III, i.e. that the doping concentration dependence of the annealing rate of the E defects is related to the position of the Fermi level. This was made clear by determining the profiles of the E_2 and E_3 traps after the annealing had been performed around 500 K in reverse-biased junctions: the defects had annealed only in the bulk and not in the space-charge

region. This was not observed by Lang (1977) because he used samples with too low a dopant concentration in which the Fermi level at the annealing temperature is much deeper than the energy level of the E_1 trap whose charge state seems to control the annealing rate.

The variation of the annealing rate of E_2 and E_3 with the doping concentration can be quantitatively accounted for using a normal 'ionisation-enhanced mechanism' (Bourgoin and Corbett 1978). In such a mechanism, the annealing rate r is a linear combination of the annealing rates of the defects r_e and r_f in the empty and filled states respectively, the coefficients being related to the fraction f of the occupied states:

$$r = r_e (1 - f) + r_f f.$$

The fraction f is calculated from the value of the associated energy level. For E_2: $E_c - 45$ meV (the energy level of E_1) and the experimental results (Pons 1981, Aukerman and Graft 1962, Lang *et al* 1976, Kimerling and Lang 1975) are fitted correctly using the following rates: $r_e = 7 \times 10^{-6}\,s^{-1}$ and $r_f = 3 \times 10^{-3}\,s^{-1}$ (see figure 6); for E_3: $r_e = 0$, $r_f = 6 \times 10^{-4}\,s^{-1}$, $E_c - 0.29$ eV.

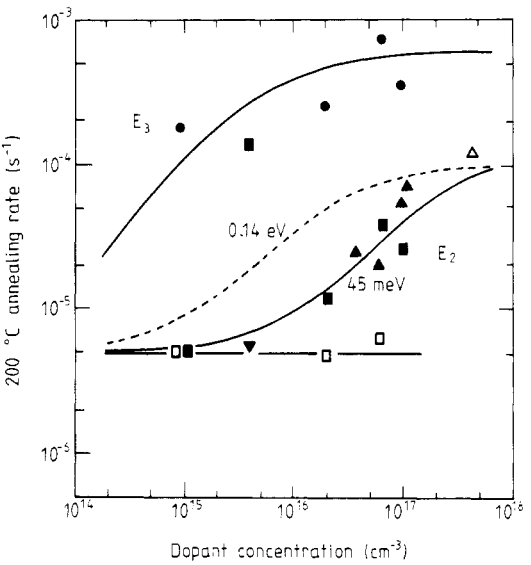

Figure 6. Rates of annealing of the E_2 and E_3 traps as a function of the doping concentration. For E_2 traps ■ denotes our results and we also plotted the annealing rate of E_2 in the space-charge region (□); the results of Aukerman and Graft (1962) (▲) and Lang *et al* (1976) (▼) are also plotted for comparison. For E_3 traps ● denotes our results and ■ those of Kimerling and Lang (1975). The full curves are the theoretical fits corresponding to the equation and values given in the text, using the energy level of E_1. The broken curve corresponds to the fit using the energy level of E_2.

3.4. Recombination-enhanced annealing

The effects of charge state on defect mobility, which have been now recognised for a number of years (Bourgoin and Corbett 1971) can take several aspects (Bourgoin and

Corbett 1978). An example of one of the mechanisms by which enhanced mobility occurs is the 'normal ionisation-enhanced' mechanism described in the previous paragraph. In GaAs, like in other III–V compounds (Lang and Kimerling 1976) another type of mechanism enhancing defect mobility is said to be operative, which illustrates the strong electron–lattice coupling existing in such material for deep levels (see § 5). To our knowledge, the first manifestation of enhanced mobility by a charge-state effect other than the 'normal' one in GaAs has been reported by Barnes (1970) who observed the complete recovery of light emission, in a laser diode irradiated with γ rays, due to current injection. The direct evidence for this effect was later given by Lang and Kimerling (1974) and Lang *et al* (1976) on the E_3 and E_2 traps. These authors demonstrated that the annealing rate of E_3 is proportional to the rate of recombination of electron–hole pairs on the associated level, from a careful analysis of the variation of this annealing rate versus the current injected in the diode.

The authors argued that the driving effect is the liberation of phonons when the defect captures a hole, i.e. the so-called 'energy released' mechanism (Bourgoin and Corbett 1978). Such a mechanism indeed accounts quantitatively for the variation of the activation energy associated with the annealing of E_3 since they said that this energy drops from 1.4 eV to 0.34 eV under injection, i.e. from a quantity equal to the energy liberated by hole trapping on the E_3 level (at $E_c - 0.29$ eV, the forbidden gap is 1.36 eV). In the case of the E_2 trap, they said that the result should be similar but that a direct demonstration has not been possible because the electron capture cross-section is too large compared with the hole capture cross-section and no saturation of the annealing rate versus current density could be reached.

Recently, D Stievenard *et al* (unpublished) performed a systematic study of the annealing rates of E_3, E_4 and E_5 versus injection level at different temperatures. This study allows the change in the activation energies and pre-exponential factors associated with the annealing of the traps as a function of the injected current density to be deduced. Several interesting features are found. First, E_4 is not at all enhanced by current injection (a difference of behaviour between E_3, E_5 and E_4 is also noticeable in the variation of their introduction rate versus the energy of irradiation (Pons *et al* 1980b) and in the fact that they anneal thermally with slightly different rates (Pons *et al* 1980a)). Second, the variation of the activation energies with the current density is similar for E_3 and E_5. This indicates that the enhanced annealing of E_5 is driven by the same mechanism as for E_3. Third, the activation energy associated with the enhanced annealing of the E_3 traps decreases linearly with the injected current density and reaches values far lower than the 0.34 eV found by Lang and Kimerling (1975).

Lang and Kimerling (1975) argued that this enhancement induced by carrier injection is the result of a recombination event at the defect and not from the accompanying changes in the average charge state, i.e. the so-called Bourgoin mechanism (Bourgoin and Corbett 1972). This last mechanism occurs when the equilibrium configuration of a defect in a given charge state becomes the saddle point configuration for its migration when its charge state changes, and vice versa. For a defect which migrates in this way, it should in principle be possible to induce its mobility in the space-charge region of a junction by applying an alternative bias. Kimerling and Lang (1975) attempted this experiment by pulsing a diode at 1.7 MHz and, because they did not observe any change in the concentration of the E_3 trap, concluded that the mechanism is not the cause of the enhanced annealing. Actually, this experiment is certainly not decisive because, using such a value of bias frequency, they practically did not enhance the rate of change of charge state as compared with the rate of thermal equilibrium induced by the different

emission and capture rates. Indeed the equilibrium rate (Bourgoin 1975) is:

$$r = 2\left(\frac{1}{k_e + g_h} + \frac{1}{k_h + g_e}\right)^{-1}$$

where k_e, k_h, g_e and g_h are respectively the electron (e) and hole (h) capture (k) and emission (g) rates. For the E_3 level, at 100 °C, the rate is limited by the electron emission, i.e. $r \sim g_e \sim 3 \times 10^6\ s^{-1}$. Thus, the only proofs that it is not a Bourgoin mechanism that operates but an energy release mechanism are based on (i) the relation between activation energies for thermal and injection annealing and the position of the E_3 level in the gap which actually, as said above, is questionable; and (ii) the fact that there should be only a factor of about 10 between the annealing rates with and without minority carrier injection at 100 °C, if driven by a Bourgoin mechanism, which is somewhat less than experimentally observed.

3.5. Conclusion

These annealing experiments confirm the picture obtained in the previous section. All the E defects anneal with a first-order kinetics and, within the experimental uncertainty, with the same activation energy. This means that all these defects are related together, i.e. they anneal because of *the mobility of one single defect* which interacts with the others. The fact that the kinetics is first order is in full agreement with the conclusion of § 2. Indeed, if the primary defects are vacancy–interstitial pairs, such pairs, if they are close pairs, i.e. if the distance between the two elements of the pair is small compared with the distance between pairs, recombine with a first-order kinetics.

Long-range diffusion towards sinks in concentration large compared with the defect concentration also result in first-order kinetics. This explanation, originally proposed (Lang 1977) to account for the difference between the annealing rates in differently doped samples—the sinks being the doping impurities—can be ruled out because the dependence of the annealing rate on the impurity concentration is entirely due to a charge state effect (see § 3.3). Moreover, the pre-exponential factor in the annealing rate implies that only few jumps occur (Pons *et al* 1980a). The amount of annealing, nearly 100%, is also a strong indication that the process involves a recombination of pairs. No defect except the one associated with P_1 is formed (with a very small concentration). This implies that only very few pairs escape the recombination. Consequently, the defects associated with the E traps (and presumably the H traps although the verification for these traps is missing) should be associated with vacancy–interstitial pairs in the As sublattice. That the annealing rate depends directly on the position of the Fermi level and not on the impurity concentration is also in agreement with the fact that the annealing is independent of the nature (Si, Ge, Sn, S, Se, Te) of the dopant (Kolchenko and Lomako 1978).

Which is the mobile defect? There is a reasonable indication that it is the interstitial As_i. Indeed, nuclear magnetic resonance suggests that quenched defects are V_{As}, stable at temperature higher than 200 °C (Hester *et al* 1974). The picture of the defects provided by annealing studies is thus the following: the E and H traps are associated with As vacancy–interstitial pairs. The number of traps observed reflects the fact that there are *several configurations for these pairs* and several levels associated with one single pair (E_1 and E_2 for instance). The change in the level position associated with a pair reflects the change in the interaction energy between the elements of the pairs, due to variable

distances or to different configurations of the interstitial. The distribution in distance should also be reflected in the number of jumps the interstitials has to make in order to recombine, i.e. in the pre-exponential factor of the annealing rate. However, because this factor also contains an entropy term which can vary strongly with the lattice distortion (Lannoo and Bourgoin 1979) no real conclusion can be drawn from its value. These pairs recombine in stage III because of the interstitial mobility. Nearly all the pairs recombine because they are close pairs and only a few interstitials escape recombination and P_1 defects are formed. Consequently, the P_1 traps should be associated with complexes involving As_i or with the isolated vacancy V_{As}.

The distinction between different kinds of pairs, i.e. of 'close' pairs and more 'distant' pairs, is confirmed by the recombination-enhanced behaviour. One can distinguish at least four types of pairs from the difference of behaviour of the E levels during thermal and injection annealing (this classification remains to be done for the H traps) and from their introduction rates. Since the wavefunction of an electron localised on V_{As} is expected to be localised mostly on the first-neighbour atoms, i.e. at a closer distance than the paired As_i, the effect of the interaction of this As_i should be to lower the energy level associated with V_{As}. In this picture, the higher the energy level, the less perturbed the associated V_{As}. One thus should expect the E_4 and E_5 traps to correspond to pairs having the closest distance and E_1, E_2 to a pair of the largest distance, E_3 being an intermediate case. We shall see in the next section that the characteristics of the E_1 and E_2 traps are indeed consistent with energy levels of an isolated V_{As}. However, such a picture raises the question of the difference in annealing behaviour under injection between the E_4 and E_5 traps. One way, not yet carefully attempted, to verify the existence of such a distribution in distance could be to look for the evolution of their relative concentration as a function of the irradiating energy since one expects that the proportion of distant pairs as compared with close pairs will increase with this energy. (This is apparently the case for the H_0 and H_1 traps (Pons 1983).)

An attempt has been made to verify that close vacancy–interstitial pairs indeed are formed by irradiating at a temperature higher than the temperature of stage III (Stievenard *et al* 1983). In this stage III all the pairs recombine, i.e. practically no defects escape recombination. However, the probability that a vacancy escapes recombination with its interstitial should increase with temperature. Thus, if the irradiation is performed at sufficiently high temperature, a fraction of the pairs should escape recombination and the result should be the formation of complexes by the trapping of interstitials on the various impurities contained in the material. This actually seems to occur: irradiation at ~300 °C produces a series of new traps in concentration considerably larger than the concentrations of the P traps which remain after stage III annealing; moreover, this concentration increases with increasing temperature, as expected. In addition, as discussed in § 2.4, complex defects B–As_i, C–As_i have been observed to form after room-temperature irradiation. In this case the dissociation of the V_{As}–As_i pairs and the migration of As_i should have been driven by the ionisation induced by the high flux of radiation.

Now we come to stages I and II which occur at ~250 K. We argued in § 2 that the defects which anneal in these stages are originally associated with a double displacement, i.e. to the configuration $V_{As} + V_{Ga}$. Since Ga_i is probably mobile even at 4 K (no defects are observed in the Ga sublattice; see the discussion in § 2.2) its recombination with $V_{As} + V_{Ga}$ should result in the following defects: V_{As} and (or) $V_{Ga} + Ga_{As}$. Since V_{As} is stable at room temperature, the only possible cause for this annealing stage to occur should therefore be a change of configuration of this last defect: $V_{Ga} + Ga_{As} \rightarrow V_{As}$. The

fact that two stages are observed, and not a single one, could perhaps be understood in terms of the existence of an intermediate configuration, the 'split' Ga_i in which the Ga atom is midway between the As and Ga sites:

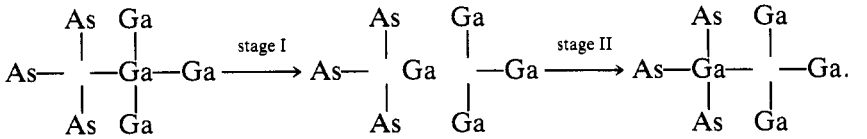

We suggest that the P_2 and P_3 traps could be the result of stages I and II annealing although this has not been experimentally verified. In this case they also should correspond to V_{As} associated with an As_i in far-distant pairs. The reason is the following: these traps anneal at higher temperature (650 K) than the E traps but with the same activation energy, because the recombination occurs through long-range migration of the interstitial. If this picture is correct, then at high temperatures the only defects left are the unpaired V_{As} related to the P_1 and P_2 traps and As_i–impurity complexes. Such a picture is the only one able to explain why the activation energy associated with P_3 annealing (the energy for P_2 has not been measured) is equal to the activation energy associated with the annealing of the E traps (Pons *et al* 1980a). We are aware that this picture contains several assumptions which need experimental verification. We present it here because we feel that it is the most reasonable one, i.e. it reconciles all the experimental observations with the minimum of unknown parameters.

4. Defect characteristics

4.1. Introduction

Up to now, we have considered the atomic properties of the defects in order to obtain information on their nature. In this section, we shall examine their electronic characteristics which can be deduced from electrical and optical measurements. The basic electrical experiment is the measurement of a thermal emission rate and of the amplitude of the emission kinetics after the application of an electric pulse serving to refill the traps. The analysis of these experiments provides the energy level and the electrical capture cross-section of the trap. In an optical experiment, the ionisation rate under optical excitation at given flux and wavelength is measured; in this case a threshold energy for optical ionisation is deduced which can be different from the energy level deduced from electrical experiments.

Both optical and electrical measurements can also provide information on the coupling with the lattice and on the defect wavefunctions. The temperature dependence of the electrical capture cross-section and the analysis of the optical ionisation cross-section as a function of wavelength are particularly interesting in this respect. The effect of some excitations like strong electric and magnetic fields, pressure (Wallis *et al* 1981, Ren *et al* 1982, Kumagai *et al* 1982) or of alloy composition (Lang *et al* 1977, Kravchenko and Prints 1979) can also be very informative. As we shall see such experiments have been performed on some of the irradiation-induced traps in GaAs.

If the capture cross-section is temperature independent, the activation energy of the thermal emission rates, as deduced from DLTS experiments for instance, is in fact the enthalpy for ionisation of the associated level. The total free energy can only be obtained through detailed balance from the determination of both the emission and capture rates

at the same temperature. The entropy for ionisation of the level, deduced from the difference between the total free energy and the enthalpy, includes the electronic degeneracy of the level, which cannot be separated from the defect entropy.

The capture rates and the electrical cross-sections can be derived rather accurately for majority carrier traps from a measurement of the fraction of traps which emit carriers after they have been filled by an electric pulse of a given duration. For minority carrier traps this technique cannot be easily applied because it is difficult to evaluate correctly the concentration of injected minority carriers, whatever the injection technique is.

In the case of large capture cross-sections (σ_e), when the free-carrier concentration (n) cannot be decreased sufficiently, the rate of filling $\sigma_e v n$ (v is the carrier velocity) can be very fast so it becomes impossible to measure it directly by the usual capacitance technique. A possible way to overcome this difficulty is to use fast microwave devices such as MESFET on the gates of which very short pulses can be applied. In this case, the transient emission of the traps is detected as a transient in the channel resistance. An illustration of such a possible technique used to apply filling pulses of the order of ns will be described in § 4.3. When the rate of filling is still faster than the time constant of the circuit (usually composed of the capacitance of the sample diode in series with the 50 Ω impedance of the pulse generator) it is still possible to measure σ_e. For this, one uses the fact that the free-carrier concentration does not vary as a step function at the edge of the space-charge region but that there is a transition region (the Debye free-carrier tail) in which the carrier concentration, and correspondingly the filling rate, decreases (Stievenard *et al* 1985a, b, Grimmeiss *et al* 1980, Pons 1980, 1984b).

As to the optical cross-sections they are obtained using the so-called DLOS (for 'deep level optical spectroscopy') technique (Chantre *et al* 1981) monitoring the initial time derivative of the emission transients during optical excitation.

4.2. Electrical energy levels

The values of the energy levels associated with the E and H traps, given in tables 1 and 2, were first determined by Lang and Kimerling (1975). The results obtained subsequently are practically in agreement with the first values reported other than for the traps E_1 and E_2. Only the H_0 trap was detected and measured later by Pons (1983).

The study of the emission rates of the traps E_1 and E_2 is especially difficult because of the strong enhancement of these emissions by the electric field (see § 4.4). The Arrhenius plots of the emission rates of E_1 and E_2 are given in figures 7 and 8, respectively. These plots have been obtained using both capacitive and current transients from temperature scans as well as from transients recorded at stabilised temperatures. The recording of transients at fixed temperatures was used to verify that they were perfectly exponential. The measurements were performed in a material containing 9×10^{14} cm^{-3} free electrons, using filling pulses of weak amplitude in order to eliminate any electric field enhancement of the emission rate. Because the Arrhenius plots obtained cover five orders of magnitude, the activation energies and apparent capture cross-sections σ_a (obtained from the pre-exponential factor of the emission rate) are determined with a good accuracy. Note that σ_a for E_2 is very large (10^{-13} cm^{-2}); this value has been confirmed (see § 4.3) by a careful study of the filling kinetics in the Debye free-carrier tail.

The activation energies that we have determined for E_1 and E_2 are significantly different from the values determined by Lang and Kimerling (1975) as well as from the 'best' values (0.13 eV and 0.20 eV, respectively for E_1 and E_2) deduced from a

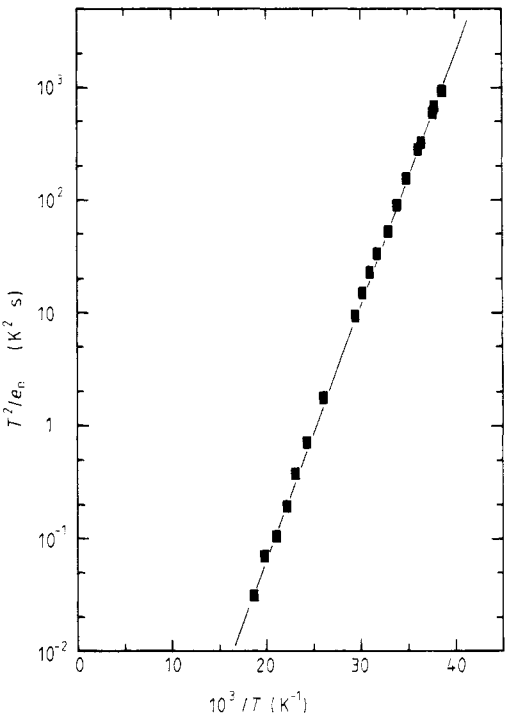

Figure 7. Arrhenius plot of the emission rate of trap E_1 for a negligible electric field. $E = 45$ meV, $\sigma = 2.2 \times 10^{-15}$ cm^2.

comparison of his DLTS determination with Hall effect data, so that we find it necessary to re-examine this comparison here. The more extensive Hall measurements have been published by Brehm and Pearson (1972); these authors explained the temperature dependence of the free-electron concentration in their irradiated samples as the manifestation of the introduction of three energy levels located at 0.130 eV, 0.170 eV and 0.310 eV below the conduction band. In order to check whether these data are really inconsistent with out DLTS data (with energy levels at 0.045 eV, 0.140 eV and 0.29 eV respectively for E_1, E_2 and E_3), we have simulated their experiment, assuming that the irradiation introduces defects with the energy levels we have determined. To make this simulation, we need the charge states of these levels, which cannot be deduced from DLTS experiments.

From the orders of magnitude of the capture cross-sections (see § 4.3), we inferred that E_2 is donor-like (10^{-13} cm^{-2}), while E_1 is acceptor-like (2×10^{-15} cm^2). E_3 is also assumed to be acceptor-like. We must immediately notice that such charge states for the traps are not inconsistent with the fact that the effect of the irradiation is to remove the free electrons in n-type material. Indeed, a concentration of defects associated with E_1, E_2 large with respect to the doping concentration will quench the Fermi level between the E_1 and E_2 energy levels, reducing the free-electron concentration, at least below room temperature. However, we must recognise that it would be impossible in this case to pin the Fermi on deeper energy levels such as the E_3 level which in fact has been observed by Brehm and Pearson. So we must assume that deep acceptor levels are also introduced (and we know from § 2 that other electron traps and hole traps are also introduced in large concentrations) to reconcile the assumed charge states of the E_1,

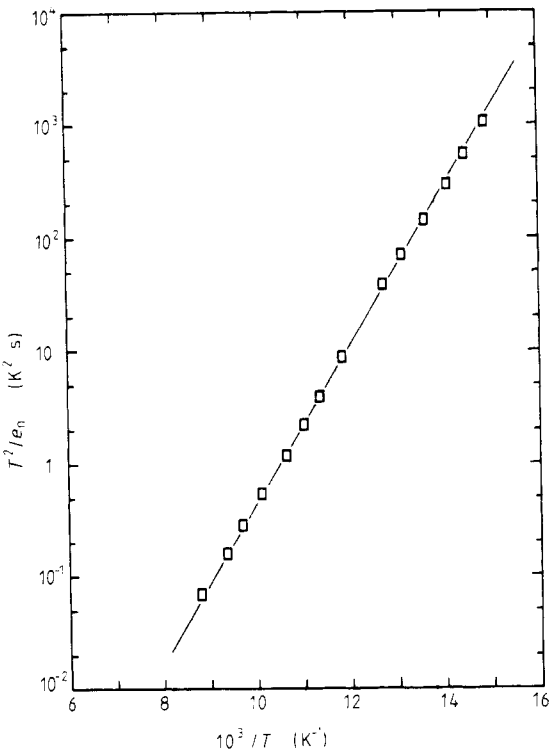

Figure 8. Arrhenius plot of the emission rate of trap E_2 for a negligible electric field. $E = 140$ meV, $\sigma = 1.2 \times 10^{-13}$ cm^2.

E_2 traps with the data of Brehm and Pearson. In order to observe the E_3 level, the concentration of deep acceptor states is required to be larger than the concentration of E_2 minus the concentration of E_3. The result of such a simulation shows that the agreement of this picture with the data of Brehm and Pearson is quite fair. In fact, our simulation shows that in such a complex situation involving three deep levels with close energy levels, any value of activation energy can be deduced from Hall effect data in the range 0.050 eV to 0.300 eV, depending on the relative concentrations of the centres and of the shallow donors.

This fair agreement shows that the Hall data are wholly consistent with the energy levels determined by DLTS. However, it must not be taken as a proof that E_2 is indeed donor-like since the same agreement was obtained assuming that it is acceptor-like. We just show that the donor-like character of E_2, inferred from its very large capture cross-section, is not inconsistent with Hall effect data. Finally, note that the levels found by Kalma *et al* (1973) at $\simeq E_c - 0.02 \pm 0.02$ eV and by Kolchenko and Lomako (1976) at $\simeq E_c - 0.04$ eV must be related to E_1.

4.3. Electronic capture cross-sections

Only a few measurements have been performed, probably because of the experimental difficulty. Bulk material or epitaxial layers of doping lower than $\sim 10^{15}$ cm^{-3} are still difficult to obtain; with such a level for the doping, the capture time constants are lower than 20 ns for capture cross-sections higher than 10^{-15} cm^2 and it is difficult to apply such

short pulses on a capacitive charge of typically 100 pF. This is unfortunate because the apparent cross-section—as deduced from the extrapolation of the Arrhenius plot of the emission rate—is identical to the true capture cross-section only if the latter is not temperature dependent and if the ionisation entropy is zero. Thus, a direct measurement of the cross-section is necessary to allow the determination of the correct variation of the energy level versus temperature.

The capture rate of E_2 was found to be very fast, even in the epitaxial layer with the lowest dopant concentration available (9×10^{14} cm^{-3}), and impossible to measure using the usual technique. An attempt has been made to use field-effect transistors as samples, on the gate of which very short filling pulses can be applied. It is however immediately recognised that standard microwave FETs cannot be used here, because of the too high value of the dopant concentration in the channel ($\sim 10^{17}$ cm^{-3}), which would remove the advantage of using short pulses. Special FETs have therefore been fabricated for our purpose with lightly doped channels ($\sim 2 \times 10^{15}$ cm^{-3}) and large gates (30×150 μm^2) (because of the rather large depth of the space-charge region). Although these had degraded microwave performances, it was nevertheless possible to apply pulses of 1 ns without too severe distortions of the rise and fall times. As demonstrated by Zylbersztejn *et al* (1979), DLTS experiments on these devices can be carried out by monitoring the transient channel resistance after the application of the pulse on the gate. The irradiated FETs exhibit the usual E traps. Despite the gain of about two orders of magnitude in capture rates compared with more conventional techniques, it was again impossible to determine directly the capture rate of E_2, but only to set the lower limit to 10^{-14} cm^2 consistent with the apparent capture cross-section (2×10^{-13} cm^2). It was, however, possible to deduce this cross-section using another method, which takes advantage of the edge region of the space-charge region where the free-carrier concentration decreases. Several experimental methods have been proposed to exploit this situation. We have used the method proposed and subsequently analysed in detail by Pons (1980, 1984b). In this technique the DLTS signal at constant temperature (temperature of the peak maximum) is plotted as a function of the refilling pulse amplitude, for different values of the pulse duration. Some typical results are shown in figure 9. The curves are

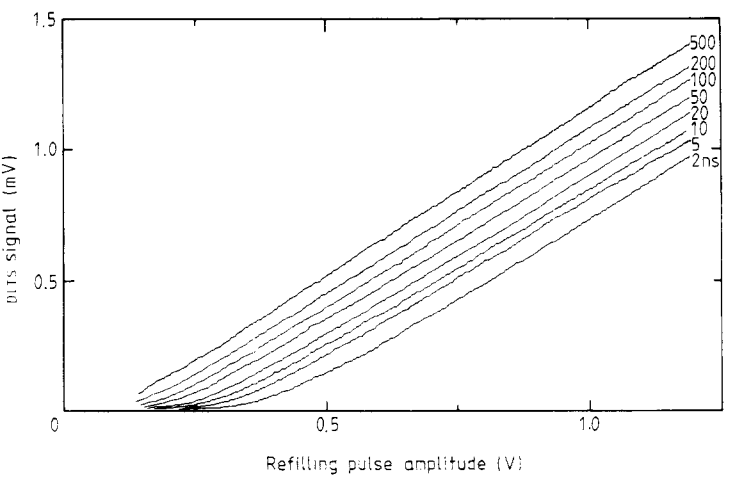

Figure 9. Variation of the transient amplitude versus the amplitude of the filling pulse for the trap E_2, for different values of the filling pulse duration marked on the curve. $T = 106$ K, gate bias = 1.0 V.

quasi-parallel and their slopes are not observed to decrease even for the 2 ns pulse duration, which indicates that the bulk capture time constant is much shorter than 2 ns. These curves are quasi-linear and their linear extrapolations provide threshold voltages increasing from about 0.1 V to 0.4 V when the pulse duration decreases from 500 ns to 2 ns. It is possible to show that the change of this threshold with pulse duration is only a function of the bulk capture time constants, all the other parameters being independently known. In figure 10 we give a typical fit from which we deduce that the bulk capture time constant for E_2 is about 2×10^{-11} s; the full curves in this figure are theoretical curves calculated for different time constants, which allows one to see the accuracy that can be obtained from such experiments.

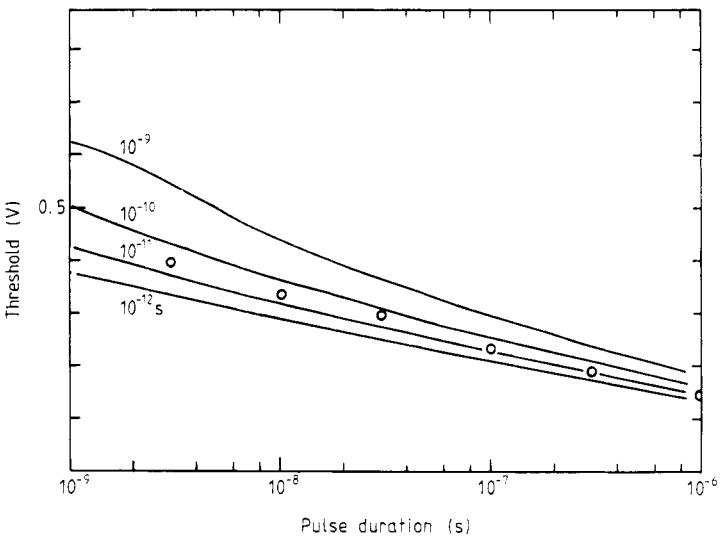

Figure 10. Determination of the capture time constant from threshold voltages measured for various values of the pulse duration. The full curves are calculated for the capture time constants indicated on the curves. $T = 95$ K, gate bias $= -1.0$ V.

This accuracy is not good enough really to study the temperature dependence of this capture cross-section which was found to be of the order of 2×10^{-13} cm^2, in perfect agreement with the apparent capture cross-section. From detailed balance and measurement of the emission time constants at the same temperatures it was possible to deduce the free-energy level for E_2 (given in figure 11). It is identical to the activation energy of the emission rate, which gives an entropy for ionisation quite negligible (as expected in this temperature range).

The irradiated FETs have also been used to measure the capture cross-section of E_3. In the case of this trap, the capture rate is low enough to be determined directly. For these measurements, we measured the slope of the curves of the DLTS signal amplitude versus pulse amplitude as a function of the pulse duration. This allows us to get rid of the capture in the edge region (Pons 1984b) and thus to obtain very accurately the capture rate in the bulk neutralised region only. The results are displayed in figure 12. The capture cross-section is found to be thermally activated with an energy equal to 80 meV, in agreement with the previous measurements of Henry and Lang (1977),

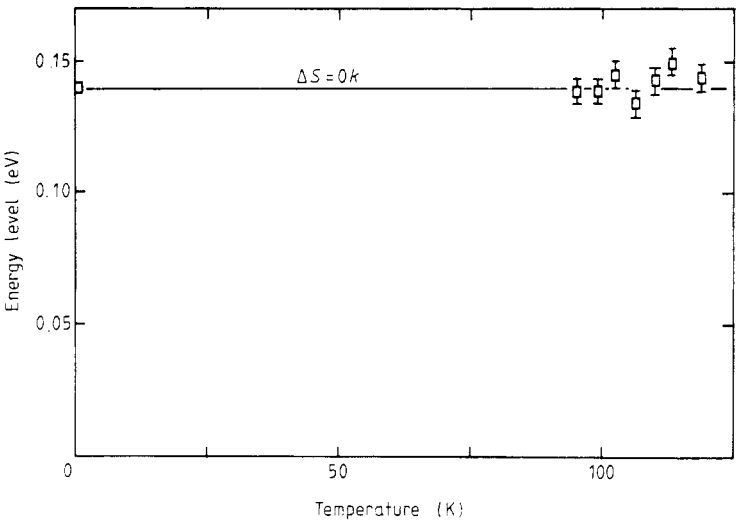

Figure 11. Variation versus temperature of the energy level of the trap E_2 which shows that this level is fixed relative to the bottom of the conduction band.

who found an activation energy of 100 meV. This is also in agreement with recent measurements by Stievenard *et al* (1985a) who used another indirect method based on the decrease of the capture rates in the edge region.

From the obtained capture cross-section and from the emission rates at the same temperatures, it is possible to get the temperature variation of the energy level, as

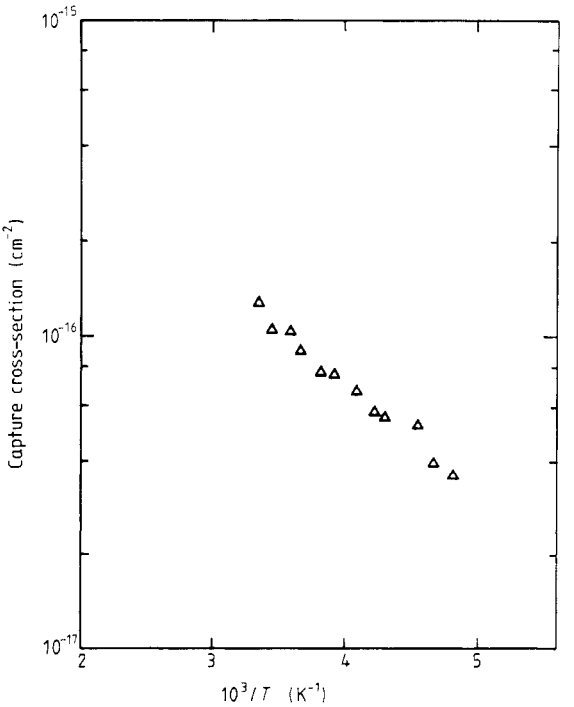

Figure 12. Variation of the electron capture cross-section of the trap E_3 versus temperature.

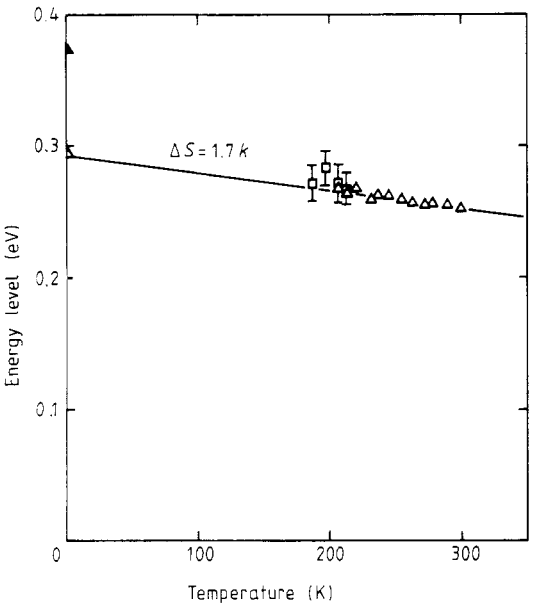

Figure 13. Variation versus temperature of the energy level of the trap E_3, relative to the conduction band, as deduced from the detailed balance relationship and from the emission and capture rates measured at the same temperature.

deduced from the detailed balance principle. The result is shown on figure 13; this temperature variation can be interpreted as resulting from an enthalpy and an entropy for ionisation equal respectively to 0.295 eV and 1.7 k in the temperature range 180–300 K.

The capture rate of electrons by the trap E_1 is very slow and can therefore easily be determined with accuracy. However, as was first noticed by Lang *et al* (1976), the refilling kinetics differs markedly from an exponential with a single time constant. A detailed experimental study of this refilling kinetics has been performed (D Pons, unpublished, Pons and Bourgoin 1985). The cross-section for E_1 which is measured at low temperature should also be equal to the apparent one, i.e. 2.2×10^{-15} cm^2. This result is in agreement with the fact that E_1 and E_2 are associated with the same defect (see § 2): these cross-sections have the order of magnitude expected if σ_{E_2} corresponds to the capture of a first electron and σ_{E_1} to the capture of a second electron. The process by which carriers get trapped on the E_1 level is different from the usual process of capture of free electrons by a trap because at the temperature (<30 K) at which the capture can be measured, only a very few electrons are delocalised in the conduction band. The electrons being localised on the donor impurities, their trapping on defect sites occurs through hopping from impurity sites to the nearest defect sites. Such a process, of which direct evidence has been found for the first time, has been called hopping capture (D Pons, unpublished). The rate of capture is characteristic of the overlap between the wavefunctions of the donor and of the defect. Because there is a random distribution of donors and of defects, the capture rate also presents a distribution. A complete theory of this process has been developed (Pons and Bourgoin 1985), which is in quantitative agreement with the observations, namely the temperature dependence of the distribution of capture rates (increasing the temperature provokes the thermal excitation of electrons in the con-

duction band so that the free-carrier capture gradually overcomes the hopping capture) and the effect of a magnetic field (which shrinks the donor wavefunction and weakens the overlap with the trap wavefunction and therefore the capture probability).

The fact that the cross-section of E_3 is thermally activated, a behaviour which is also found for other defects in other III–V compounds (Henry and Lang 1977), can be understood in terms of electron–lattice coupling. This multiphonon capture process has been a matter of considerable work (for references and a general treatment see Bourgoin and Lannoo (1983), ch 6). In the case of E_2, whose cross-section is not thermally activated, and very large ($1.2 \times 10^{-13}\,cm^2$) one would think that the associated electron–lattice coupling is very weak. However, this is apparently not the case (see § 4.4 and § 4.5); but we must not exclude the possibility that the configuration coordinate diagram for this trap is such that the parabola which represents its electron plus phonon energy in the filled state crosses the parabola of the empty state near the minimum of the last one, which represents a rather large lattice distortion and which would result in a negligible activation energy for the capture. We shall see in the next two sections that the existence of such strong electron–lattice coupling is verified and can be made more quantitative.

4.4. Optical cross-section

An optical cross-section σ_0 for a transition between a defect level and a band has for characteristics an energy level E_0 and an oscillator strength β (see Bourgoin and Lannoo 1983, ch 4). When the transition occurs towards several bands (Γ, X and L for instance in the case of the conduction band) the optical cross-section can be approximated to the sum of the cross-sections corresponding to each band:

$$\sigma_0 = \sum_i \beta_i \, \sigma_0^i \, (m_i^* , E_0^i)$$

where m_i^* is the effective mass in the band i (Chantre *et al* 1981). A fit of an optical spectrum to such an expression provides E_0^i, once corrected for the electron–phonon coupling, the respective oscillator strengths β_i of the transitions towards the extrema of the different bands, the Franck–Condon parameter d_{FC} and the extension in space α of the wavefunction associated with the defect.

The DLOS technique, based on the observation of the kinetics associated with the ionisation of a defect level under optical excitation, is a unique way to get the optical spectrum associated with one single localised level because it can be performed at low enough temperatures where the thermal emission rate is negligible and because the correlative use of DLTS allows the separation of the optical emission rate associated with a distinct trap.

As shown in table 1, for the only traps for which this type of measurement has been performed, i.e. E_1, E_2 (Loualiche *et al* 1984b) and E_3 (Chantre *et al* 1981), Franck–Condon shifts of the order 0.2–0.4 eV are deduced. Since the effective frequency which drives the displacement of the nearest neighbours of a defect is expected to be the transverse acoustic frequency ($\hbar\omega = 10$ meV), the corresponding amount of displacement Δq in a single configuration coordinate, given by $d_{FC} = \frac{1}{2} M\omega^2 \Delta q^2$, is 0.4–0.6 Å.

As already noticed in the preceding section, it is *a priori* difficult to accept these large numbers, at least for E_2. Indeed, since the two traps E_1 and E_2 correspond to two

different charge states of the same defect, the spatial extension α of the wavefunction should increase with the order of the excited state, i.e. $\alpha_{E_1}^{-1} > \alpha_{E_2}^{-1}$ and the value of d_{FC} should decrease accordingly, which is not experimentally verified.

As for the results concerning the E_3 trap, the value deduced for d_{FC} (~0.2 eV) is in poor agreement with that derived from electrical cross-section measurements (~0.1 eV). We think that such a difference illustrates the fact that the values derived for d_{FC} must be considered as only being semiquantitative. This can also be seen by comparing d_{FC} with the difference between thermal and optical ionisation energies.

4.5. Phonon-assisted tunnelling emission

The effect of the intensity of the electric field present in a junction on the emission rates of electrons from localised levels was soon observed. Since the electric field strength varies linearly in the space-charge region there is a distribution of emission rates e associated with a single level, which strongly distorts the emission kinetics. The study of this effect can be performed easily using DLTS since such a technique allows the emission associated with one single deep level to be monitored in a narrow depth of the space-charge region where the electric field can be assumed to remain constant (Makram-Ebeid 1980). Previously, this field effect was usually explained in terms of lowering of the potential emission barrier by the electric field, the so-called Poole–Frenkel effect (Frenkel 1938). This explanation indeed applies to shallow levels. However, for deep levels, often the field enhancement of the emission rate varies exponentially with T^{-1} and with the electric field and is too strong to be accounted for quantitatively by the Poole–Frenkel effect. It was finally recognised that this phenomenon involves a tunnelling effect modified to account for the electron–phonon coupling (Vincent 1978) and a theory of phonon-assisted tunnelling emission was developed (Pons and Makram-Ebeid 1979) and subsequently refined (Makram-Ebeid and Lannoo 1982a, b) to fit quantitatively the experimental observations. The semiclassical image of the quantum mechanical treatment is as follows. Because of the electron–lattice coupling the electronic energy of a bound state is a (linear) function of the lattice deformation around the defect, schematised by a single configuration coordinate Q. Since Q oscillates at the phonon frequency ω, with an amplitude related to the total energy of the phonon mode involved, there is a distribution of quasi-levels from which the localised charge can be emitted in the band, via elastic tunnelling. Thus the emission rate is the probability of finding the charge trapped on a quasi-level, times the tunnelling emission probability (at high enough temperatures the thermal emission process should be added). Thus, the enhancement of the emission is a function of the Franck–Condon shift d_{FC}.

Concerning the irradiation-induced defects, a quantitative study of this field enhancement has only been performed on E_3 (Pons and Makram-Ebeid 1979, Makram-Ebeid and Lannoo 1982a, b) leading to the respective values $d_{FC} = 75 \pm 20$ meV, and 125 ± 10 meV. This is in reasonable agreement with the value deduced from the activation energy of the capture cross-section, but not with that deduced from the optical ionisation cross-section. The electric field enhancement of the emission rates for the traps E_1 and E_2 has been also experimentally studied (D Pons 1984, unpublished). In particular, the emission from the E_2 level has been observed at the lowest temperatures (4.2 K) which means that the electric field enhancement of its emission rate can be larger than 100 orders of magnitude at this temperature. No attempt has yet been made to compare these results with the phonon-assisted tunnelling theory of Makram-Ebeid and Lannoo (1982a, b). Such a quantitative study for the traps E_1 and E_2 should therefore

be very helpful in order to verify the very large values of d_{FC} deduced from optical cross-section studies.

4.6. Comparison with theory

A comparison of the experimental results with theory is not yet very useful to verify the defect identification for several reasons. First, the theory (local density approximation) is not yet really able to predict quantitatively (as long as it will not reproduce correctly the bandgap energy) energy levels (Lannoo 1984) and lattice distortions and relaxations to which the energy levels are very sensitive and we think that the defects observed have a strongly distorted configuration. Since we argue that the traps E_1 and E_2 are related to V_{As} which is the less perturbed by the interstitial, it is tempting to compare the characteristics of these traps with those expected for the isolated V_{As}. This has been done by Loualiche *et al* (1984a, b) who suggested a reasonable way to deduce, from the experimental characteristics, the value an energy level would have with zero distortion, a value which can be compared directly with theory. They found that the E_1 and E_2 levels fit the prediction of the available theoretical calculations (Bachelet *et al* 1981) for the transitions $2-/-$ and $-/0$ states respectively. Unfortunately, at the energy position where they predict the $0/+$ charge state, there is no level observed. However, the value of the electron capture cross-section measured for E_2, apparently very large for a neutral state, can be justified (Lannoo 1985).

Several authors attempted to identify the energy levels associated with the vacancy from a study of their dependence on pressure or alloy composition (Lang *et al* 1977, Wallis *et al* 1981). Because a vacancy wavefunction is expected to be made of Bloch waves of the valence and (or) conduction bands, depending on its nature, the way an energy level follows these bands when the forbidden gap changes—with pressure or alloy composition—is in principle a way to deduce the nature of the wavefunction characteristic of this level and, consequently, the nature of the defect itself (Ren *et al* 1982). Unfortunately, in practice, this is much more complicated because the wavefunction has to be described by a linear combination of the Bloch waves of the various minima of a band. This difficulty is well illustrated by the conclusion drawn by Lang *et al* (1977) who argued that the E_3 trap was associated with V_{Ga} because it follows the top of the valence band; actually, this trap also follows closely the X_c minimum of the conduction band (Wallis *et al* 1981). In fact, all the E_1, E_2, E_3 and E_4 traps shift in a similar way relative to this minimum.

5. Conclusion

The picture of the defects produced by electron irradiation in GaAs which can be derived from the studies of their production (§ 2) and annealing behaviour (§ 3) is the following: they are primary defects in the As sublattice, i.e. made up of V_{As} and As_i which are distributed in pairs. All the E traps are associated with these pairs. This should also be the case for the H traps although certain information is still missing so we cannot draw a firm conclusion. Only the E_9 and E_7 traps are associated with a more complicated defect resulting from two adjacent displacements (presumably the association of V_{As} with a Ga_{As} antisite). No defects are observed in the Ga sublattice because the V_{Ga}, Ga_i pairs recombine immediately after their creation, even at the lowest temperature, presumably because of Coulomb attraction.

Other defects can actually be produced, at least following irradiation at room temperature and above in special conditions, namely when the migration of As_i can be induced by hole injection. Then, the migrating As_i which escape recombination with a V_{As} form complexes with impurities such as B and C. In some cases they exchange their interstitial sites for the substitutional sites of impurities on Ga sites, resulting in the formation of As_{Ga} antisites.

There are apparently at least four different kinds of V_{As}–As_i pairs that are produced, as can be deduced from the slight differences between the annealing and creation behaviours. This explains the large number of traps observed. They are associated with different levels because their configurations, namely the distance between the two elements of a pair, are different. As to the H traps, it should be very interesting to compare their annealing behaviours with these four categories of defects.

All the electrical and optical characteristics of these defects point to the fact that there is a large lattice distortion around the defect (this has still to be verified for the E_4 and E_5 traps). Such a distortion is a manifestation of a strong electron–lattice coupling, characterised by the so-called Franck–Condon shift, detected by the difference between electrical and optical excitation energies but also by the way the electrons are captured on the defect site and by the electric field enhancement of electron emission. Such a phenomenon is not surprising if the observed traps are associated with the vacancy since it is well known from a study of the vacancy in silicon that such a defect undergoes various types of Jahn–Teller distortions as a function of its charge state. The situation could be similar if the interstitial is only a weak perturbation on the electronic states of V_{As}, as seems to be the case for V_{Zn}–Zn_i pairs in ZnSe according to Watkins (1975). However, we feel that the situation is different in GaAs since the levels associated with the different pairs are distributed all over the forbidden gap: if the energy levels of a pair can be described in terms of V_{As} levels perturbed by the presence of a nearby As_i, this perturbation should be strong. The E_1 and E_2 traps are associated with pairs at the longest distance and it is well possible that in this case As_i interacts only slightly with the V_{As} since their characteristics are the ones expected for the isolated V_{As}.

In conclusion, the large amount of work that has been devoted to this subject is just sufficient to get an idea of the nature of the defects produced and to determine their electronic and atomic characteristics. However, much more remains to be done if one wants really to reach the point where a direct identification will be possible. For this, one should rely, in addition to EPR (especially at high frequency) with which several centres other than the antisite can be detected (J von Bardeleben, unpublished), also on ENDOR and techniques providing defect symmetry, i.e. coupling two or more polarised excitations.

Acknowledgments

This work was partly supported by Centre National d'Etudes des Télécommunications (84.6B.035.0079) and Ministère de la Recherche et de la Technologie (82.A.1355 and 82.A.1481).

References

Arnold G W 1966 *Phys. Rev.* **149** 679
—— 1969 *Phys. Rev.* **183** 777

Arnold G W and Gobeli G W 1968 *Radiation Effects in Semiconductors* ed. F L Vook (New York: Plenum) p 435
Aukerman L W and Graft R D 1962 *Phys. Rev.* **127** 1576
Bachelet G B, Baraff G A and Schluter M 1981 *Phys. Rev.* **24** 943
Baraff G A, Kane E O and Schluter M 1980 *Phys. Rev.* B **21** 5662
Baraff G A and Schluter M 1984 private communication
Barnes C E 1970 *Phys. Rev.* B **1** 4735
Beall R B, Newman R C, Whitehouse J E and Woodhead J 1984 *J. Phys. C: Solid State Phys.* **17** 2653
Bourgoin J C 1975 *Radiation Damage Processes in Materials* ed. C H S Dupuy (London: Noordhoff) p 339
Bourgoin J C and Corbett J W 1971 *Trans. IEEE Trans. Nucl. Sci.* **NS-18** 11
—— 1972 *Phys. Lett.* **38A** 135
—— 1978 *Radiat. Effects* **36** 157
Bourgoin J and Lannoo M 1983 *Point Defects in Semiconductors: Experimental Aspects* (Berlin: Springer)
Brailovskii E Y and Brudnyi V N 1974 *Sov. Phys.–Semicond.* **8** 619
Brehm G E and Pearson G L 1972 *J. Appl. Phys.* **43** 568
Brozel M R and Newman R C 1978 *J. Phys. C: Solid State Phys.* **11** 3135
Brozel M R, Newman R C and Totterdell D H J 1975 *J. Phys. C: Solid State Phys.* **8** 243
Chantre A, Vincent G and Bois D 1981 *Phys. Rev* B **23** 5335
Corbett J W and Bourgoin J C 1975 *Point Defects in Solids* vol 2, ed. J A Crawford and L M Slifkin (New York: Plenum) ch 1
Corbett J W and Watkins G D 1965 *Phys. Rev.* **138** A555
Eisen F H 1964 *Phys. Rev.* **135** A1394
Farmer J W and Look D C 1980 *Phys. Rev.* B **21** 3389
Frenkel J 1938 *Phys. Rev.* **54** 657
Garrido J, Custano J L and Pigueras J 1981 *Phys. Status Solidi* a **65** 103
Goswami N K, Newman R C and Whitehouse J E 1981 *Solid State Commun.* **40** 473
Grimmeiss H G, Ledebo L A and Meyer E 1980 *Appl. Phys. Lett.* **36** 307
Henry C H and Lang D V 1977 *Phys. Rev.* B **15** 989
Hester R K, Sher A, Soest J F and Weisz G 1974 *Phys. Rev.* B **10** 4262
Ikoma T and Takikawa M 1981 *Japan. J. Appl. Phys.* **20** L591
Jeong M, Shirafuyi J and Inuishi Y 1973 *Japan. J. Appl. Phys.* **12** 109
Kalma A H and Berger R A 1972 *IEEE Trans. Nucl. Sci.* **NS-19** 209
Kalma A H, Berger R A and Cesena R A 1973 *Radiation Damage and Defects in Semiconductors* (Inst. Phys. Conf. Ser. 16) p 364
Kennedy T A, Faraday B J and Wilsey N D 1981 *Bull. Am. Phys. Soc.* **26** 255
Kimerling L C and Lang D V 1975 *Lattice Defects in Semiconductors* (Inst. Phys. Conf. Ser. 23) p 589
Klein C A 1968 *J. Appl. Phys.* **39** 2029
Kolchenko T I and Lomako V M 1976 *Sov. Phys.–Semicond.* **9** 1153
—— 1978 *Radiat. Effects* **37** 67
Kravchenko A F and Prints V Y 1979 *Sov. Phys.–Semicond.* **12** 952
Kumagai O, Wünstel K and Jantsch W 1982 *Solid State Commun.* **41** 89
Lang D V 1974 *J. Appl. Phys.* **45** 3023
—— 1977 *Radiation Effects in Semiconductors* (Inst. Phys. Conf. Ser. 31) p 70
Lang D V and Kimerling L C 1974 *Phys. Rev. Lett.* **33** 489
—— 1975 *Lattice Defects in Semiconductors* (Inst. Phys. Conf. Ser. 23) p 589
—— 1976 *Appl. Phys. Lett* **28** 248
Lang D V, Kimerling L C and Leung S Y 1976 *J. Appl. Phys.* **47** 3587
Lang D V, Logan R A and Kimerling L C 1977 *Phys. Rev.* B **15** 4874
Lannoo M 1984 *J. Phys. C: Solid State Phys.* **17** 3137
—— 1985 *Proc. 13th Int. Conf. Defects in Semiconductors (San Diego, USA) 1984* (The Metallurgical Society of the AIME) p 221
Lannoo M and Bourgoin J C 1979 *Solid State Commun.* **32** 913
—— 1981 *Point Defects in Semiconductors: Theoretical Aspects* (Berlin: Springer)
Loualiche S, Guillot G, Nouilhat A and Bourgoin J C 1982a *Phys. Rev.* B **26** 7090
Loualiche S, Guillot G, Nouilhat A and Lannoo M 1984a *Solid State Commun.* **51** 509
—— 1984b *Phys. Rev.* B **30** 5822
Loualiche S, Nouilhat A, Guillot G, Gavand M, Laugier A and Bourgoin J C 1982b *J. Appl. Phys.* **53** 8691
Makram-Ebeid S 1980 *Appl. Phys. Lett.* **37** 464
Makram-Ebeid S and Lannoo M 1982a *Phys. Rev. Lett.* **48** 1281

—— 1982b *Phys. Rev.* B **25** 6406
Martin G and Makram-Ebeid S 1983 *Acta Electros.* **25** 133
Meyer B K, Spaeth J M and Scheffler M 1984 *Phys. Rev. Lett.* **52** 851
Mircea A and Bois D 1979 *Defects and Radiation Effects in Semiconductors* (Inst. Phys. Conf. Ser. 46) p 82
Newman R C and Woodhead J 1984 *J. Phys. C: Solid State Phys.* **17** 1405
Özbay B, Newman R C and Woodhead J 1982 *J. Phys. C: Solid State Phys.* **15** 581
Pajot B 1984 private communication
Pons D 1980 *Appl. Phys. Lett.* **37** 423
—— 1981 *Defects and Radiation Effects in Semiconductors* (Inst. Phys. Conf. Ser. 59) p 269
—— 1983 *Physica* B **116** 388
—— 1984a *J. Appl. Phys.* **55** 2839
—— 1984b *J. Appl. Phys.* **55** 3644
Pons D and Bourgoin J C 1981 *Phys. Rev. Lett.* **47** 1293
—— 1985 *Proc. 13th Int. Conf. Defects in Semiconductors (San Diego, USA) 1984* (The Metallurgical Society of the AIME) p 989
Pons D and Makram-Ebeid S 1979 *J Physique* **40** 1161
Pons D, Mircea A and Bourgoin J 1980a *J. Appl. Phys.* **51** 4150
Pons D, Mooney P M and Bourgoin J C 1980b *J. Appl. Phys.* **51** 2038
Poulin F and Bourgoin J C 1980 *Revue Phys. Appl.* **15** 15
—— 1981 *Recent Developments in Condensed Matter Physics* vol 3, ed. J T Devreese (New York: Plenum) p 83
Ren S Y, Dow J D and Wolford D J 1982 *Phys. Rev.* B **25** 7661
Rezazadeh A A and Palmer D W 1985 *J. Phys. C: Solid State Phys.* **18** 43
Steeples K, Dearnaley G and Stoneham A M 1980 *Appl. Phys. Lett.* **36** 981
Stein H J 1969 *J. Appl. Phys.* **40** 5300
Stievenard D, Bourgoin J C and Pons D 1983 *Physica* B **116** 394
Stievenard D, Lannoo M and Bourgoin J C 1985a *J. Appl. Phys.* to be published
—— 1985b *Solid State Electron.* to be published
Thommen K 1968 *Phys. Rev.* **174** 938
—— 1970 *Radiat. Effects* **2** 201
Vincent G 1978 *Thesis* University of Lyon
Wagner R J, Krebs J J, Stauss G H and White A M 1980 *Solid State Commun.* **36** 15
Wallis R H, Zylbersztejn A and Besson J M 1981 *Appl. Phys. Lett.* **28** 698
Watkins G D 1965 *Radiation Damage in Semiconductors* (Paris: Dunod) p 97
—— 1975 *Lattice Defects in Semiconductors* (Inst. Phys. Conf. Ser. 23) p 338
Weber E R, Ennen H, Kaufmann U, Windscheil J, Schneider J and Wosinski T 1982 *J. Appl. Phys.* **53** 6140
Whitehouse J E, Goswami N K and Newman R C 1981 *J. Phys. C: Solid State Phys.* **14** L319
Woodhead J and Newman R C 1981 *J. Phys. C: Solid State Phys.* **14** L345
Wörner R, Kaufman U and Schneider J 1982 *Appl. Phys. Lett.* **40** 141
Zylbersztejn A, Bert G and Nuzillat G 1979 *Gallium Arsenide and Related Compounds 1978* (Inst. Phys. Conf. Ser. 45) p 315